Probing Dark Matter through Cosmic Gamma Rays

A thesis submitted in partial fulfilment of the requirements for the degree of

Masters of Science

in

Physics

By

Gautham Kumar Jayakumar

20MSP1023

Under the Guidance of

Prof. Ranjan Laha, CHEP, IISc. - Bangalore

Prof. Satyanarayana Kumar, Dept. of Physics, School of Advanced Sciences, VIT

Division of Physics

School of Advanced Sciences

Vellore Institute of Technology

May 2022

Abstract

In this masters thesis, we investigate the possibility of dark matter decay as a source for high energy cosmic gamma rays. Particularly looking at channels of heavy Dark matter decay. In lieu of the new sub-PeV diffuse gamma ray event from the Tibet AS_γ collaboration a few studies have been published in this area. We attempt to build towards recreating some of the results from these papers. We go through all the necessary ingredients to calculate our photon flux for the proposed model. We calculate the flux at production using the PPPC4DM spectra including the electro-weak bremmstrahlung and inverse Compton corrections. Finally we compare with observations to set our difference estimator. Using available values of the 95% CL limit of these estimators we try to impose stronger cutoffs on the lifetimes of heavy dark matter mass through some prominent decay channels. We discuss our results in contrast to the recent work we've reviewed in this area and comment on the possibility of seeing these signals in future dark matter searches.

Contents

List of Figures

List of Tables

Abbreviation

eV	Electron Volt
GeV	Giga Electron Volt
PeV	Peta Electron Volt
Tibet AS	Tibet Air Shower
PPPC	Poor Particle Physicist Cook Book
DM	Dark Matter
ID	Indirect Detection
CL	Confidence Limit
MOND	Modified Newtonian Dynamics
GR	General Relativity
CDM	Cold Dark Matter
kpc	kilo parsec
SM	Standard Model
dec	Decay
N	Decay Event count
l.o.s	Line of Sight
MW	Milkyway
WIMP	Weakly Interacting Massive Particles
VHDM	Very Heavy Dark Matter
LAT	Large Area Telescope
NFW	Navarro Frank White
Ein	Einasto
SL	Starlight

IR	Infrared
CMB	Cosmic Microwave Background
EW	Electro-Weak
ICS	Inverse Compton Scattering
N.P.	New Physics

Symbols and Notations

Ω	Energy Density Fraction
ρ_c	Critical Energy Density
ρ_Λ	Dark Energy Energy Density
$\rho_D M$	Dark Matter Energy Density
ρ_b	Baryon Energy Density
ρ_r	Radiation Energy Density
$R(t)$	Universal Radius
$\langle \sigma v \rangle$	Annihilation Cross-Section
p	Pressure
$\mathbf{G}_N$	Gravitational Constant
H, h	Hubble Parameter
P_f	Final state momentum
P_i	Initial state momentum
δ	delta function
E_i, E_p	Initial particle Energy
Λ	Cosmological Constant
χ	Dark Matter Particle
Γ	Decay Width
τ	Lifetime
$\Delta\Omega$	Angular region Solid Angle
ψ	Sky direction
γ	Gamma or Γ Ray
$r_\odot$	Solar Radius

$\rho_{\odot}$	Galactic energy density
s	Line of Sight Distance
f	Final state (used typically as subscript)
ℓ	Galactic plane latitude
b	Galactic plane longitude
$n(t)$	Number density
e^{+}	positron
e^{-}	electron
γ_b	Background photon
$\sigma_{\gamma\gamma}$	Pair Production cross section
α	fine-structure constant
m_e	electron mass
L	Attenuation distance
T_{CMB}	Cosmic Microwave Background Temperature
P_{IC}	Inverse Compton power spectrum

1 Introduction

Dark matter studies have been one of the most prominent forefronts of modern physics research. But very little is known of it. Since scattering cross sections of DM are very small, and event rates to low to be detected in a collider, one looks into the sky to find sources. While gravitational observation techniques are very good, it is simply not enough. Indirect detection of dark matter through study of high energy gamma rays have gained more relevance in recent years. Entering into this fray is the Tibet AS_γ survey with it's recent discovers of sub-PeV diffuse gamma rays. We look at a particular recent work in this area [12],which posit that DM decay could fit the data from a particular sky section of the survey. We expand on that through this thesis and use our theory to recreate the new found upper limits on dark matter lifetimes.

In chapter 1, a literature survey, we trace all recent and past evidences for dark matter and our chosen standard cosmological model. Then we walk through how that affects our choice of milkyway structure and DM density profiles. Then we provide a brief introduction to DM indirect detection techniques, especially those pertaining to dark matter decay.

In chapter two we walk through cosmic gamma rays and explore the findings from the Tibet survey. We delve a little bit into the inner working of the Tibet detector and explain our choice of sky section selection and provide the energy bins to be used.

In chapter three we put everything together to calculate our total photon flux. We explore our choice of DM density profile. Showcase how line of sight integration works for localized gamma ray events and set up the attenuation factor. Then we discuss influences to the gamma ray spectrum from secondary process and make necessary modifications to the prompt photon flux.

In chapter 5, we go through our final calculation and talk about how the flux expression in chapter 4 is handled in terms of the PPPC4DMID spectra. We elaborate on the χ^2 estimator and display our results of dark matter lifetimes for various decay channels.

In chapter 6 we discuss the comparison between our simplified study and recently published work and comment on any discrepancies found throughout our assumptions. We also elucidate on the possibility of finding these dark matter signals in future searches.

2 Dark Matter: What We Know and Require

Within this chapter, I trace the story of dark matter from it's initial inception to today. Highlighting key aspects, supporting evidences and expanding on calculation techniques required further down the line.

2.1 Proof of Existence

Galactic Rotation Curves

One of the earliest and strongest evidences from dark matter is from the measure of galactic rotational curves. This was initially discovered by Fritz Zwicky in 1937[13], and then corroborated by Vera Rubin in 1962[13]. However it wasn't until 1978 that it's existence was accepted. [1]

The measurement went as follows. If luminous matter[2] is assumed to constitute all present galactic mass, then one can extrapolate the total mass from a measurement of it's brightness. This in turn allows one to plot the angular velocity of galactic material as a function of it's radius. The data however showed a slower decrease i.e., at the speed the galaxy was rotating, the stars should be flying of them. This radial decrease is shown here in fig 2.1

This deviation from theory hints at either a gravitational theory breakdown at astronomical scales or simply missing matter/mass. Under comfortable assumptions of a galactic disk and a surrounding halo(sphere) of mass, the missing matter finds good correlation between theory and data if all of this 'dark matter' only has gravitational

[1] Fritz Zwicky's initial proclamations were rejected by the community due to his lack of fraternisation with them. While Vera Rubin unfortunately suffered from gender bias. Thankfully she kept up the work and was vindicated with further evidence later on [13]

[2] stars and interstellar gas

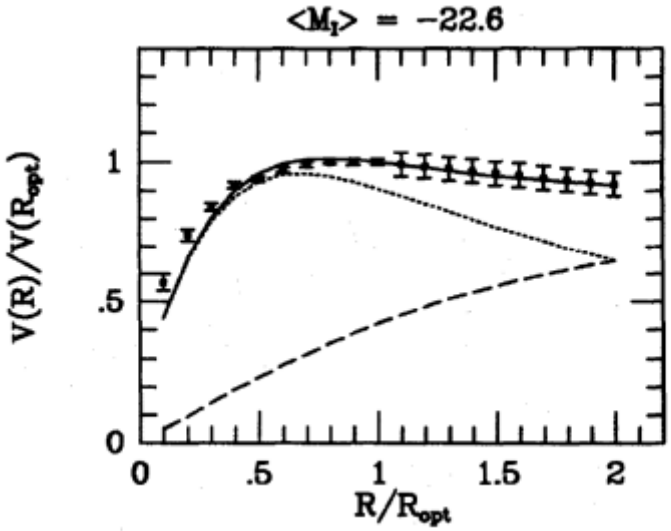

Figure 2.1: Rotation curve(points) vs expected velocity profile without DM(dotted). DM profile(dashed)[1]

interaction with visible matter.

Galactic Collisions

The best way to improve on the aforementioned evidence is to look at certain extreme astronomical events. Dark Matter needs to be valid over large cosmological length scales in order to supersede MOND like theories. Galactic cluster formations, are extreme astronomical events where galaxies participate in collision mergers. During this the intergalactic gases interact emitting X-ray radiation. A recent example of this can be seen in merger of galaxy clusters 1E2215 and 1E2216 [14]. The Chandra observatory's X-ray data has been interpolated with a radio image from GMRT India [14] with an optical image from the Sloan digital sky survey in [14]. The red part of fig 2.2 describes the X ray shockfront produced by the gas interactions. Using the background galaxies as a gravitational lens one can figure out the bulk co-moving mass of these structures.

Figure 2.2: Cluster Merger, composite image.source: Nasa-Chandra observatory

There is a clear discrepancy in the movement of the major mass of the event compared to the X-ray interaction. This is a particularly difficult task to explain through MOND [15]. Astro-particle dark matter however is easily able to Occam's razor this problem.

The most famous event under this proof is probably the bullet cluster galaxy. However there have been some contradictory events as well like the Abell 520 merger [16]. This has been explored extensively in[17, 18]. Luckily, Clowe.et.al [19] has been able to clarify these claimes and mitigate the differences.

CMB and the Energy density fraction

An important piece of evidence lies in abundance calculations through measurements of Cosmic Microwave Background radiations(CMB) [20]. The universe's energy density can be defined through,

$$\Omega = \frac{\rho}{\rho_c} \tag{1}$$

where, $\rho_c = 1.06 \times 10^4\ eVcm^{-3}$. This arises from the choice of a flat universe.[3] The CMBR refers to radiation produced from primordial processes of our universe's inception. It is the afterglow of the big bang. The radiation is currently found in the microwave range with a peak temperature of 2.726K, similar to black body radiation. Ideally the matter-radiation distribution should be homogeneous. But due to the density perturbations created by inflation[20], the power spectra stops behaving as a typical black body. Which leads to the deviations in the measured date of the CMBR compared to our theoretical predictions. The degree of these changes helps track the relative energy densities of various matter present in the primordial soup.[4] Values of said relative measurements, setting $\Omega_{tot} = 1$, can be found in [20]

$$\begin{aligned} \Omega_\Lambda = 0.725 \pm 0.016 \quad \Omega_{DM} = 0.1126 \pm 0.0036 \\ \Omega_b h^2 = 0.0255 \pm 0.00054 \qquad \Omega_r h^2 \sim 0 \end{aligned} \tag{2}$$

These fractions also helps us delve into structure formation choices in dealing with galaxies. An important aspect of the core calculations of our work. But before we get to it, there is a need to address some basic cosmology and particle physics aspects and build from it

[3] While unfamiliar terms are introduced here, it will be elaborated further in a later section within this chapter

[4] The primordial soup refers to the plasma like state the early universe was found in [20]

2.2 Rudimentary Cosmology and Particle Physics

Cosmology

The Cosmological principle thinks of a the universe as a simple structure. Across large length scales, it is spatially isotropic and homogenous

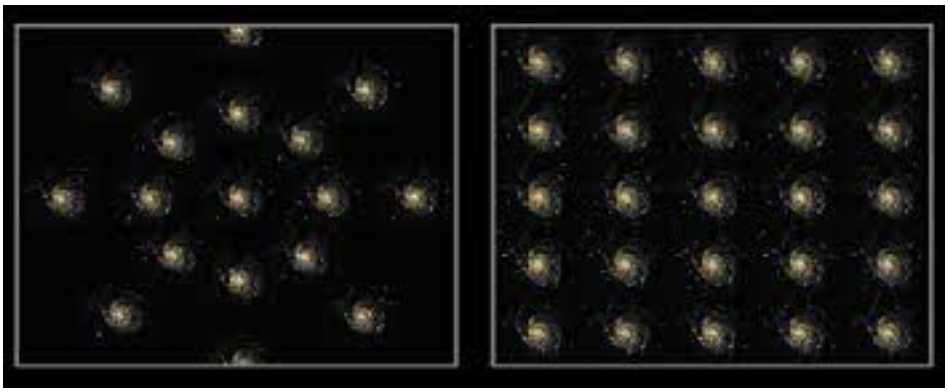

Figure 2.3: Homogenous vs Isotropic universe.[2]

In keeping with this, we can write a generalized metric for our universe known as the Friedman-Robertson-Walker(FRW) metric. This is given as, [21]

$$ds^2 = dt^2 - R^2(t)\left[\frac{dr^2}{1-kr^2} + r^2 d\Omega\right] \tag{3}$$

Notice that it is easy to see the symmetries by looking at the invariance of R, r and k under,

$$\begin{aligned} R &\mapsto \lambda^{-1} R \\ r &\mapsto \lambda r \\ k &\mapsto \lambda^{-2} k \end{aligned} \tag{4}$$

Here k is the curvature factor having values $\pm 1, 0$, depending on closed, open or flat

space. While $R(t)$ tracks the change in radius over time, it is standard practice to use a dimensionless parametrisation via a scale factor $a(t)$.

$$a(t) = R(t)/R_0 \tag{5}$$

where, R_0 is the scale of today.

The question then arises as to how to govern the evolution of this scale factor. The answer lies in the combination of Einstein's General Theory of Relativity(GR) as applied to a *perfect fluid*.[5]

The typical Einstein equation is given by [2],

$$\mathbf{R}_{\mu\nu} \;=\; 8\pi\mathbf{G}_N(\mathbf{T}_{\mu\nu} - \frac{1}{2}\mathbf{g}_{\mu\nu}) \tag{6}$$

Here, $\mathbf{R}_{\mu\nu}$ is the Ricci Tensor, $\mathbf{T}_{\mu\nu}$ is the energy-momentum tensor, whose trace becomes very important for our work and finally $\mathbf{g}_{\mu\nu}$ is the metric tensor. While an intricate and somewhat exhausting solution to the to this equation is warranted, it is beyond the scope of this thesis. Thus it is easier to get the trace of our energy-momentum tensor for perfect fluids in terms of energy density and pressure from [2],

$$\begin{aligned} T^{\mu}_{\nu} &= diag(-\rho, p, p, p) \\ &= -\rho + 3p \end{aligned} \tag{7}$$

This gives rise to the state equation,

$$p = w\rho \tag{8}$$

[5] A perfect fluid is something that only requires it's mass/energy density and pressure to characterise it [2]

Imposing the time invariance symmetry, one gets

$$\begin{aligned} \frac{\dot{\rho}}{\rho} &= -3(1+w)\frac{\dot{a}}{a} \\ \implies \rho &\propto a^{-3(1+w)} \end{aligned} \tag{9}$$

Here the w parameter is a dimensionless number and has certain special values depending on what dominates our cosmic fluid. This helps us describe the evolution of density of the various entities present in our universe [2]. This leads to the predictions and measurements we landed earlier on in Eqn2.

Going back to the Einstein equation and writing it out explicitly as per the indices gives us, For $\mu\nu = 0, 0$:-

$$\frac{\ddot{a}}{a} \;=\; -4\pi \mathbf{G}_N(\rho + 3p) \tag{10}$$

and for the other three identical tensor trace elements (Isotropy):-

$$\frac{\ddot{a}}{a} + 2(\frac{\dot{a}}{a})^2 + 2\frac{k}{a^2} \;=\; 4\pi \mathbf{G}_N(\rho - p) \tag{11}$$

Putting the above equations together and re-writing $(\frac{\dot{a}}{a})^2 \equiv H^2$, *Hubble Parameter* we get,

$$H^2 = \frac{8\pi \mathbf{G}_N}{3}\rho - \frac{k}{a^2} \tag{12}$$

This is known as the Friedmann equation[22]. A useful parametrization, which ties in back to the CMB measurements is to rewrite,

$$\rho_{crit} \equiv \frac{3H^2}{8\pi \mathbf{G}_N} \tag{13}$$

This combined with the definition of the density fraction/abundance gives us

$$\Omega - 1 \; = \; \frac{k}{H^2 a^2} \tag{14}$$

From here we can comfortably infer what was mentioned in the subsection on CMB measurements.

Particle Physics

Since the crux of this work is dependent on dealing with DM decay and subsequent annihilation/scattering events, it is good to refresh a little about cross-sections and decay widths. We will develop on the base concepts introduced here in further sections within this chapter.

- **Scattering Cross Section**:-

  Consider the initial state of a 2-1 or 2-many process. Where a particle of mass,velocity and number density(m_1, v_1, n_1) hits another unique particle (m_2, v_2, n_2)[6] Then the likeliness of an event or N events is given by,

  $$dN = \sigma(v_1 n_1) n_2 dV dt \tag{15}$$

  Here σ is the **scattering cross section** While this is a simplistic ansatz, the inner workings of writing a *differential*/scattering cross section in a Lorentz-invariant fashion is not within the scope of our thesis however a good reference can be found here [23]. We will simply borrow the idea that the scattering cross section for a

[6]These can be a beam of particles also. We assume uniformity if that is the case.

generic n-particle final state can be written as :-

$$d\sigma \ = \frac{1}{4I} \mid M_{fi} \mid^2 d\Phi^{(n)} \ , \ where \tag{16}$$

$$d\Phi^{(n)} = (2\pi)^4 \delta^{(4)}(P_i - P_f) \prod_{i=1}^{n} \frac{d^3 p_i}{(2\pi)^3 (2E_i)} \tag{17}$$

Here, $d\Phi^{(n)}$ is the differential cross-section, M_{fi} is the appropriate matrix element corresponding to the final state and I is the flux factor.

- **Decay Width**:-

  A decay typically refers to a 1-2 or 1-many process. This is studied using the probability to decay to n final states over a time T. Thus the decay rate

$$d\Gamma \ = \ \frac{1}{T} dP \tag{18}$$

  which using our handy technique from [23] gives us,

$$d\Gamma = \frac{1}{2E_p} \mid M_{fi} \mid^2 d\Phi^{(n)} \tag{19}$$

The total decay width is given by,

$$\Gamma = \int d\Gamma \tag{20}$$

2.3 Dark Matter Structure and the MilkyWay

From our praeludium on cosmology from the previous section we know that ρ[7] of radiation scales as a^{-4}[8] while matter scales at a^{-3}. This would imply that at some point in time, the universe started to be matter dominated and eventually formed structures. So at this point of genesis so to speak, gravitational-dark matter interactions become very important. The story goes as this, the universe which was initially perfectly cosmological[9], eventually becomes perturbed enough from the spark set by inflation [24, 25, 26, 27, 28] . Dark matter grabs hold of these perturbations, ties them down gravitationally and makes the cosmic dust settle into the astronomical design we know of today. The big question here lies in the Lorentzian nature of dark matter at this epoch.

Through running large scale many body monte carlos of gravitationally communicating open quantum systems [29, 30, 31, 32, 32, 33, 34] leads to two separate schools of thought on this matter.

- **Cold Dark Matter(CDM)**:- This takes stable, non-relativistic candidates at the formational epoch leading to a bottom up approach, where there is a proliferation of small scale bubble-like formations unto the large astronomical structures of today over cosmological time scales. Combining this with a non-zero cosmological constant[10] gives us the standard model of cosmology or the ΛCDM model. GeV scale DM is a prevalent candidate of these relics.

- **Relativistic DM**:-

  This leads to a reverse hierarchical structure formation, where smaller galactic

[7] energy density
[8] scale factor
[9] homogeneous and isotropic
[10] A non-zero cosmological constant is a popular theory used to explain the current domination of dark energy in our expanding universe [35]

structures evolve from the deconstruction of larger conglomerates as time passes. This is referred to as "Hot Dark matter". This typically consists of DM candidates that have masses in the eV scale. However these thermal relics aren't very prevalent in the community due to the discrepancies they raise in the timeline of galaxy formations and their measured redshifts [35].

Galactic Density Evolution

In choosing a DM model, we also intern constrain the evolution that our galaxies undergo and the density of the energy inside them. The many body simulation briefly discussed in the previous section allow us to parametrize the energy density of galaxies, particularly our own milkyway, by extrapolating from fits made to data.

The typical setup is described via :-

$$\rho(r) = \frac{\rho_0}{(\frac{r}{r_s})^{\gamma}[1 + (\frac{r}{r_s})^{\alpha}]^{\frac{(\beta-\gamma)}{\alpha}}} \tag{21}$$

Here, α, β, γ are simply numbers and r_s is the radius of scale. That is it describes the points at which the structure we are looking at goes from matter to radiation domination and vice-versa. ρ_0 is a normalization factor, defined as a constant for our Milkyway at 0.3 GeV cm^{-3} for the solar circle.[11].

Prominent groups have performed their own simulations under the ΛCDM choice, the results are tabulated below [30, 31, 32, 32, 33, 34]. This helps cut down the previous required constants and gives us an alternative approach that we will use in our

[11] $R_s c = 8.5 kpc$

calculations.

$$
\begin{aligned}
\text{NFW}: \quad \rho_{\text{NFW}}(r) &= \rho_s \frac{r_s}{r}\left(1+\frac{r}{r_s}\right)^{-2} \\
\text{Einasto}: \quad \rho_{\text{Ein}}(r) &= \rho_s \exp\left\{-\frac{2}{\alpha}\left[\left(\frac{r}{r_s}\right)^{\alpha}-1\right]\right\} \\
\text{Isothermal}: \quad \rho_{\text{Iso}}(r) &= \frac{\rho_s}{1+(r/r_s)^2} \\
\text{Burkert}: \quad \rho_{\text{Bur}}(r) &= \frac{\rho_s}{(1+r/r_s)(1+(r/r_s)^2)} \\
\text{Moore}: \quad \rho_{\text{Moo}}(r) &= \rho_s \left(\frac{r_s}{r}\right)^{1.16}\left(1+\frac{r}{r_s}\right)^{-1.84}
\end{aligned}
\tag{22}
$$

Table 2.1: Relevant values for Popular DM profiles [11]

DM halo	α	r_s [kpc]	ρ_s [GeV/cm^3]
NFW	–	24.42	0.184
Einasto	0.17	28.44	0.033
EinastoB	0.11	35.24	0.021
Isothermal	–	4.38	1.387
Burkert	–	12.67	0.712
Moore	–	30.28	0.105

If we were to plot(fig 2.4) this against given data, we would observe fairly large agreement at large length scales and deviation as one gets closer to the galactic cent er. A decent study on these discrepancies for small galaxies can be found here [36]. This just points to the issue of the standard cosmological model not having accurate descriptions of our galactic centre to be able to accurately predict the distribution of it's constituent matter. Especially at smaller length scales.

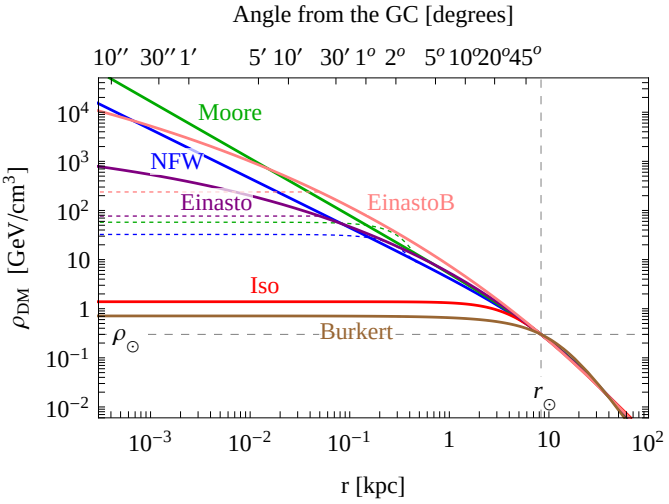

Figure 2.4: Plot of Density Evolution's for various profiles across various galactic plane rotations and distances.

2.4 Interacting Dark Matter: Decays and Light

Indirect Searches

We have already seen that observed density of dark matter is $\Omega_{DM}h^2 \simeq 0.11$. Especially considering models of DM decaying to SM particles in the weak scale known as WIMPS [37, 38, 39, 40, 41, 42].

These WIMPs are typically consistent with ΛCDM models and are thus expected to be stable on non primordial timescales. However late decays can occur via non-gravitational processes. This is a key aspect of our thesis work. Because decay into SM final states result in astrophysical fluxes. Their detection or non-detection rather allows us to constrain DM lifetimes.

A non-gravitational DM process can be any of the following as shown in fig 2.5

As shown above the Indirect searches refers to detecting dark matter properties without actually needing the initial particle in question. According to [2], it has three key ingredients.

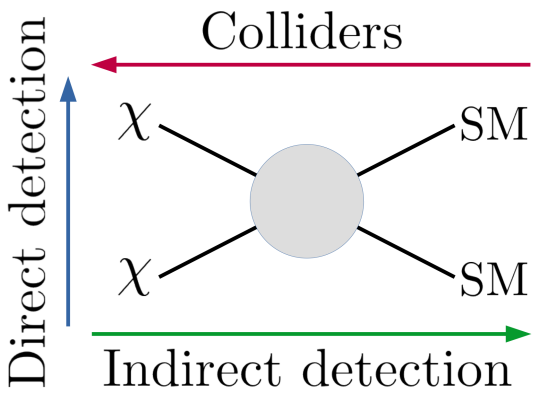

Figure 2.5: Various Non-Gravitational processes involving DM and SM fields [3]

1. Production Rates of relevant SM particles also called messengers.

2. The energy scale of these messengers. This is usually chosen by the DM model and subsequently it's mass scale.

3. The annihilation product. This is highly model dependent.

We will concentrate on Indirect Detection, especially that of DM decay.

Light from Decay

We will concentrate on Indirect Detection, especially that of DM decay.

The rate of an SM messenger for decay is given by,

$$\Gamma_{SM,dec} \simeq \left(\int_V \frac{\rho_{DM}}{m_\chi} dV \right) \times \tau_{dec}^{-1} \times N_{SM,dec} \tag{23}$$

As shown, the final state is typically some ($\chi \rightarrow SM$) Here our final SM field is light. This can happen in one of two ways,

- *Prompt* photons from the actual initial event,

- *Secondary* photons from radiative processes occurring from the stable products of the initial decay. [12]

In going about calculating the actual flux, we require combining the previous things we learned about. Any flux calculation involves a particle physics part(Final state flux), an astronomical structure piece(J decay) and combining with corrections from assumed secondary processes. Here we will introduce a simple ansatz and then elucidate it further in chapter 4.

The particle piece, in terms of the decay width is given by [43],

$$P(E_f, m_\chi) = \frac{1}{m_\chi \tau_\chi} \frac{dN_{SM}}{dE_{SM}} \tag{24}$$

The last term is a sum of the entire gamma-ray spectrum. The total flux of produced photons at given sky region and direction ψ within a solid angle $\Delta\Omega$ is,

$$\phi_\gamma = \frac{\Delta\Omega}{4\pi} \left\{ \frac{1}{\Delta\Omega} \int d\Omega \int dl(\psi)(\rho^2_{DM}) \right\} P(E_f, m_\chi) \tag{25}$$

Here, the term in curly brackets is often referred to as the J factor. In reality this is actually the "Averarge J factor", given as $\bar{J} = J(\Delta\Omega, \psi)$ [2].

J factor

The J factor is the astrophysical piece of our gamma ray flux calculation. It integrates everything present in the path the photon has to travel through along a "line of sight" from event to detector. A useful parametrization of the J-factor along with differential

[12] In calculations this is usually included as radiative corrections to the initial flux

decay flux is given here [11]

$$\frac{d\Phi_\gamma}{d\Omega\, dE} = \frac{r_\odot}{4\pi}\frac{\rho_\odot}{M_{\rm DM}} J \sum_f \Gamma_f \frac{dN_\gamma^f}{dE}, \qquad J = \int_{\rm l.o.s.} \frac{ds}{r_\odot}\left(\frac{\rho(r(s,\theta))}{\rho_\odot}\right) \qquad \text{(decay)} \quad (26)$$

Here, r is a measure of distance from the Galactic centre and is given by $r(s,\theta) = (r_\odot^2 + s^2 - 2\, r_\odot\, s\cos\theta)^{1/2}$.

Ofcourse, here the J factor is given as a function of theta , but for a localized area, it is better to use the solid angle [44] and get the average J factor integrated over a region $\Delta\Omega$ as mentioned above.

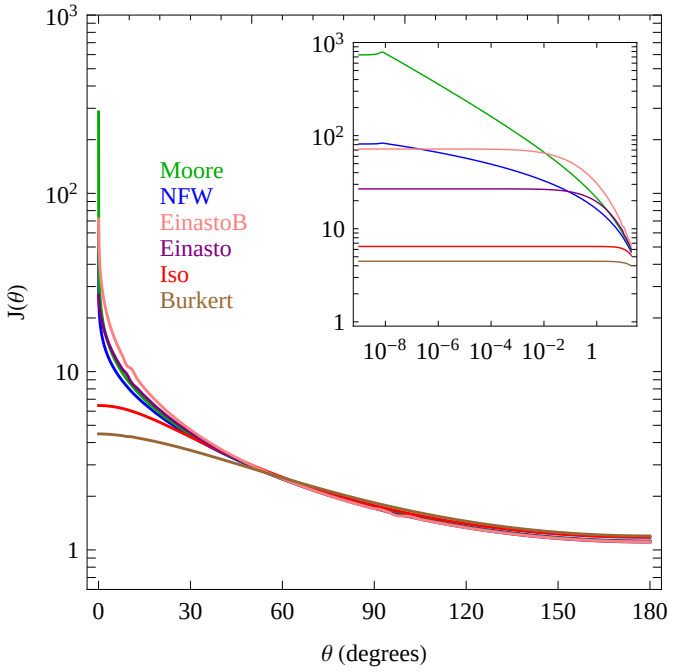

Figure 2.6: $J(\theta)$ plotted across various angles from the galactic centers across the evolution of popular density profiles

The average J factor is given as $\bar{J}(\Delta\Omega) = \left(\int_{\Delta\Omega} J\, d\Omega\right)/\Delta\Omega$. Which are modified accordingly depending on the region/type of region looked at for the event. In terms of

θ, galactic longitude b and latitude l [11]. [13]

$$\Delta\Omega = 2\pi \int_0^{\theta_{\rm max}} d\theta\ \sin\theta, \qquad \bar{J} = \frac{2\pi}{\Delta\Omega} \int d\theta\ \sin\theta\, J(\theta), \qquad \text{(disk)}$$

$$\Delta\Omega = 2\pi \int_{\theta_{\rm min}}^{\theta_{\rm max}} d\theta\ \sin\theta, \qquad \bar{J} = \frac{2\pi}{\Delta\Omega} \int d\theta\ \sin\theta\, J(\theta), \qquad \text{(annulus)}$$

$$\Delta\Omega = 4 \int_{b_{\rm min}}^{b_{\rm max}} \int_{\ell_{\rm min}}^{\ell_{\rm max}} db\, d\ell\ \cos b, \qquad \bar{J} = \frac{4}{\Delta\Omega} \iint db\, d\ell\ \cos b\, J(\theta(b,\ell)), \qquad (b \times \ell \text{ region}) \tag{27}$$

[13] Galactic polar coordinates (d, ℓ, b) can be written as

$$x = d\cos\ell\cos b, \qquad y = d\sin\ell\cos b, \qquad z = d\sin b$$

where $\vec{x} = 0$ is Earth, d is distance to event; the Galactic Center is at $r_\odot$, and the plane corresponds to $z \approx 0$.[11] Consequently $\cos\theta = x/d = \cos b \cdot \cos\ell$.

3 Cosmic Rays and Detectors

Physicist Victor hess, discovered cosmic rays in 1912 [3] At an altitute of 5300 meter, he measured ionisation rates via hot air balloon. The measured data showed a three-fold increase as compared to that at sea level. This would mean that ionising radiation was somehow entering through the atmosphere from extra-terrestrial or rather cosmic sources.

Several observations of these cosmic rays have been made over the years and hold prominent clues to explain our universe. The high energy cosmic ray is mostly hadronic (protons(89%)) [45]. A typical cosmic ray will hit earth by reacting with atoms in the upper atmosphere. This reaction typically leads to the creation of highly reactive pions. Depending on the charge of the pions, we can either get a shower of hadrons, gamma rays or further processes which lead to muonic or Cherenkov radiation.

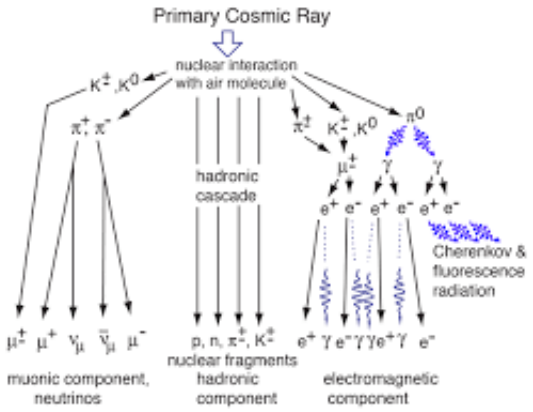

Figure 3.1: Hadronic and Leptonic Processes involved in cosmic rays

3.1 Cosmic Gamma Rays

As indicated at the end of the previous section, light from dark matter, i.e., cosmic gamma rays form an important part of non-gravitational dark matter studies. These cosmic gamma rays are produced through hadronic or leptonic processes [46, 47, 48, 49, 50].

Coming to our DM scenario, assuming a WIMP like cross section, the predicted mass is 100 $GeV \sim TeV$ [51]. This would involve high energy gamma rays around the same scale. But for such an energetic process, the actual amount of final states generated are equally numerous. Luckily gamma rays are electrically neutral and aren't put off course by extra galactic magnetic fields and quite easy to trace back to source. Thus these gamma rays are called messengers and are found across the entire universe sky as seen in fig 3.2. Something we'll make use of extensively in our calculations[52].

Gamma Rays are characterised by their really small wavelenghts. Typical sources are some of the most thermally and kinetically active objects in the universe such as neutron star, supernovae , black hole horizons etc. This can also occur through cosmic-ray (CR) interaction with interstellar gas. The mean free path of these aforementioned photon energies help probe the high energy astrophysics of our Milkyway[53, 54, 55, 56, 57, 8, 58].

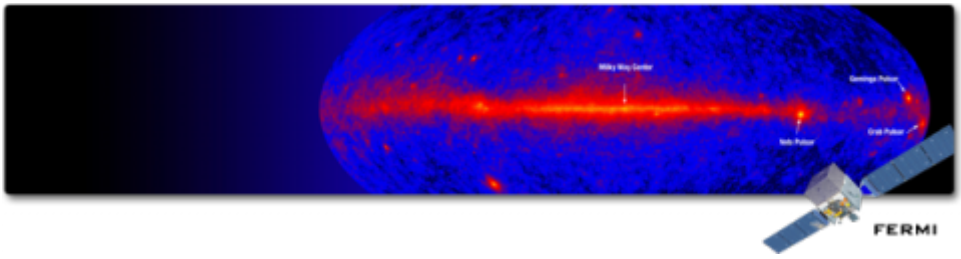

Figure 3.2: Composite gamma ray sky[4]

Unfortunately, these small wavelength also make them quite difficult to detect. Typ-

ical detectors work based on Compton scattering by use of crystalline block structures.

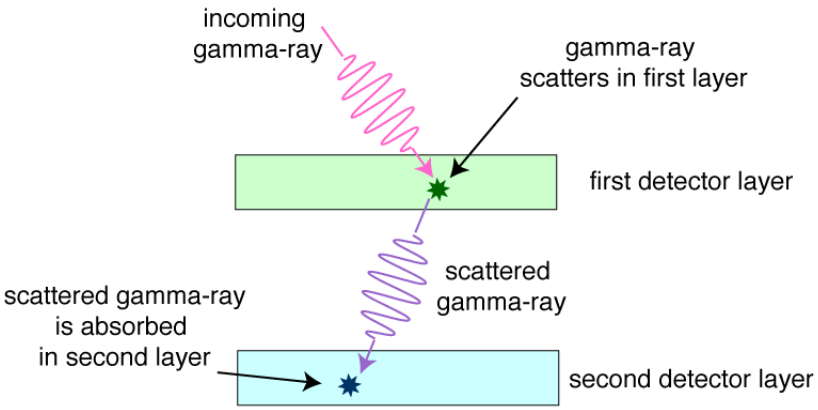

Figure 3.3: Basic Schematic of a crystalline Compton detector[5]

An important process involved in cosmic gamma rays are the fact that the high energy ones interact further and annihilate in the electron-positron shower[52] These showers will futher produce particle at faster than the speed of light in air leading to Cherenkov radiation, that is typically detected via use of ground based detector arrays or atmospheric ones [52].

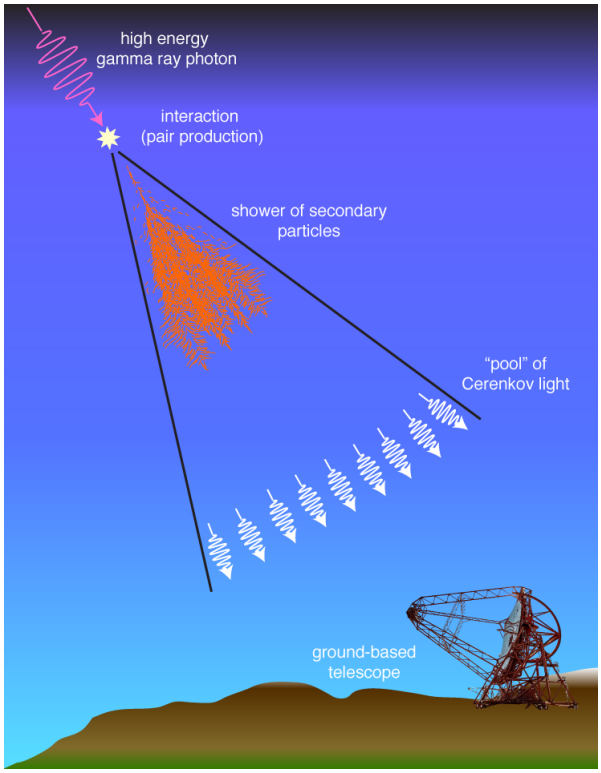

Figure 3.4: Schematic of a surface based Cherenkov detector. [5]

Newer detectors combine these above ground arrays with an underground muon detectors in order to differentiate the gamma rays from other cosmic rays. These showers have large differences in their signature when compared to muon lifetimes as they pass through the detector. Refer fig 3.5

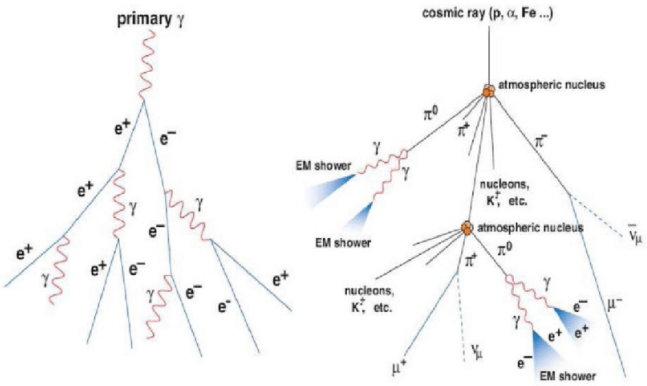

Figure 3.5: Proton vs Photon Showers. [6]

3.2 The Tibet AS$_\gamma$ Detector

The Tibet AS$_\gamma$ Collaboration, a China-Japan joint experiment has recently uncovered the highest gamma ray signal to this date from the Crab nebula. This sub-PeV diffuse gamma ray will open new avenues in Astro-particle physics [8].

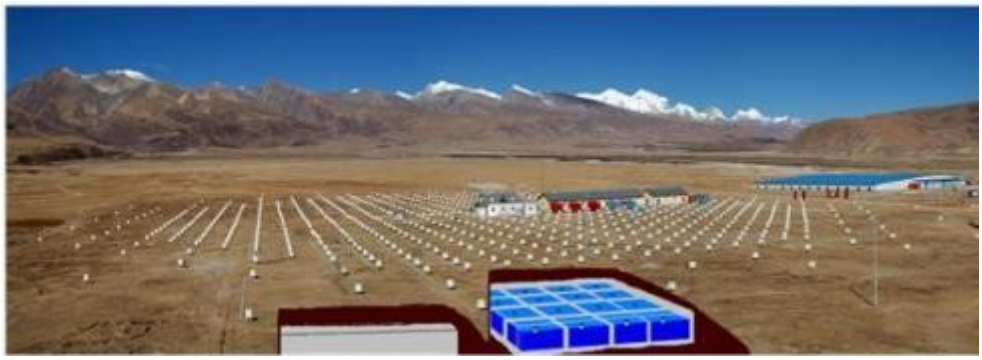

Figure 3.6: TibeT AS$_\gamma$ Survey, surface array [7]

The survey added a new Cherenkov based detector hybridised with a muon grid under the original above ground survey in 2014[7]. This helped cut off background noise by 99.92% . They have detected several candidates above 100 TeV, with the highest at around 450 TeV. This trumps all earlier upper limits found previously in this region

[59, 60, 61].

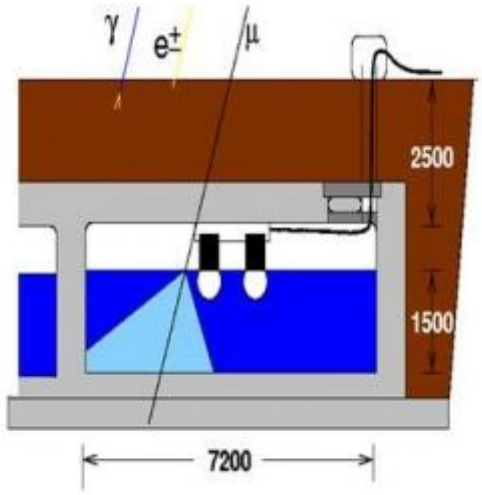

Figure 3.7: Tiber As survey, muon detector schematics[7]

These gamma rays that were detected over two major sky regions [8] prompted a revisiting to various hadronic and leptonic process that could have caused this[58, 12]. Along with the confirmation that the event is from CR interaction with interstellar gas in the Crab nebula[7] and the verification from the studies confirmed the validity of these results.

Luckily, [12] has given us the data points(energy bins) and the suitable sky region [14] for our calculations. Refer table 3.1

The graphs in fig 3.8 themselves show several fits with respect to different cosmic gamma ray models. While an intricate study of these models and their representations make for much more detailed limits as in [12], it unfortunately beyond the scope of this study. However as we borrow the choice of our sky region, we may notice that perhaps sky region (b) seems to have a much more free energy budget to include DM decay.

[14] $25° < l < 100°; \|b\| < 5°$

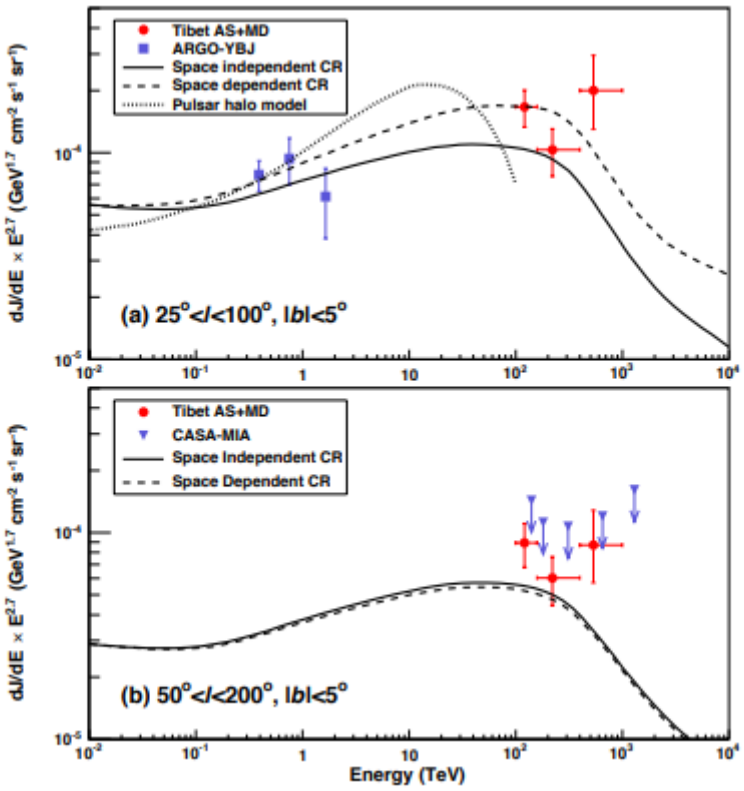

Figure 3.8: Gamma Ray event flux and Cosmic model fits from Tibet AS_γ [8]

However this is still under a single iteration of the error bar and one needs atleast 5 to be qualified as an event.

Table 3.1: Tibet AS$_\gamma$ Energy Bins [12]

Energy Bin (Tev)	Representative E (Tev)	Flux $(25^\circ < 100^\circ, \|b\| < 5^\circ)$ $(Tev^{-1}cm^{-2}s^{-1}sr^{-1})$	Flux $(50^\circ < 200^\circ, \|b\| < 5^\circ)$ $(Tev^{-1}cm^{-2}s^{-1}sr^{-1})$
100-158	121	(3.16 ± 0.64) x 10^{-15}	(1.69 ± 0.41) x 10^{-15}
158-398	220	(3.88 ± 1.00) x 10^{-16}	(2.27 ± 0.60) x 10^{-16}
398-1000	534	$(6.86 \begin{cases} +3.30 \\ -2.40 \end{cases})$ x 10^{-17}	$(2.99 \begin{cases} +1.40 \\ -1.02 \end{cases})$ x 10^{-17}

4 DM Decay as a source of Cosmic Gamma Rays

We posit that the gamma ray signal mentioned in the previous chapter can be used to explain decaying DM [62, 63, 64, 65, 66, 67].

Given the energy scale of the gamma ray signature found by the Tibet survery, we assume the DM mass to be heavy and in sub-PeV Range. Many models have been proposed in recent literature relating to this [68, 69, 70, 71, 72, 73, 74, 75, 76, 77, 78, 79, 80, 81, 82, 83, 84, 85, 86, 87, 88, 89, 90, 91, 92, 93, 94, 95, 96, 97, 98, 99, 97]. The current best constraints on these heavy DM before our core paper[12] can be found in [100, 62, 101, 102]. These use studies from Ice-Cube and Fermi-LAT. The idea here is to further develop the theory introduced in chapter one into specific equations pertinent to our scenario and do a simple recreation of the limits found in [12].

4.1 Galactic density Formalism

High energy decaying DM belongs to the ΛCDM model and thus it's halos follow the NFW/Einasto type. For our milky way galaxy, a cored DM profile[103, 104, 105] This

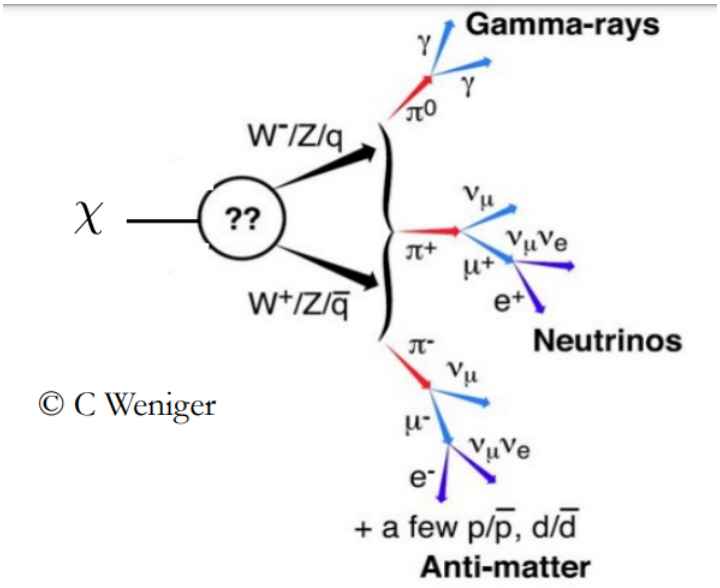

Figure 4.1: Schematic of DM decay processes [9]

gives our choice of DM density profile to be,

$$\rho_{\chi}^{Ein}(r) = \rho_{\odot}(\frac{-2}{0.17}\frac{r^{0.17} - (8.3Kpc)^{0}.17}{(20kpc)^{0}.17}) \tag{28}$$

Here , $\rho_{\odot}$ is 0.4 GeV /cm^3 is the density of our earth locality.

4.2 Prompt Photon flux and J factor

We assume an abundance of both prompt and secondary processes for our gamma ray production from our DM decay. However we will forgo the model dependent final states and look at a model independent approach involving high energy photons from unstable SM decays and stable decay via bremsstrahlung. We will begin deriving our required prompt photon flux and it's necessary ingredients by using the method given in [44]

Assume a detector area A, with a signal located at some volume V at some cylindrical coordinate in the sky with Earth as its origin. At one observable event per decay we have the spectrum of photons[15] is given as:-

$$\frac{dN_\gamma}{dEdtdV} = \left(\frac{dN_\gamma}{dE}\right)_0 \frac{A}{4\pi r^2} \times \frac{1}{2}\frac{n(\vec{r})}{\tau} \tag{29}$$

Integrating along the line of sight [16], we find:

$$\frac{dN_\gamma}{dEdtd\Omega} = \frac{A}{4\pi}\left(\frac{dN_\gamma}{dE}\right)_0 \times \frac{1}{m_\chi \tau_\chi}\int_0^\infty dr\rho(\vec{r}) \tag{30}$$

For our loaclized[17] source we integrate over the solid angle subtended by the object, to obtain the full signal from our source:

$$\frac{dN_\gamma}{dEdt} = \frac{A}{4\pi}\left(\frac{dN_\gamma}{dE}\right)_0 \times \frac{1}{m_\chi \tau_\chi}\int_0^\infty dr d\Omega\rho(\vec{r}) \tag{31}$$

Here the integral is the J factor introduced in Chapter 1. If we improve upon this and write our total flux using the averaged J factor and parametrization using galactic latitudes and longitudes. We get our total prompt flux :-

$$\frac{d^2\phi_\gamma}{dE_\gamma d\Omega}(E_\gamma) \;\; = \frac{1}{\Delta\Omega}\int_{\Delta\Omega} d\Omega \frac{1}{4\pi m_\chi \tau_\chi}\frac{dN_\gamma}{dE_\gamma}(E_\gamma)\int_0^{s_{\max}} \rho_\chi(s,b,l)ds, \tag{32}$$

Notice that we have indicated our choice of galactic disk profile in the limits involving our J factor.[18]

[15] reaching earth per volume per time

[16] The assumption that the energy of photons do not change between creation and reception

[17] intergalactic[64]

[18] The line of sight distance s and r depends on b and ℓ: $r(s,\, b,\, \ell) \,=\, \sqrt{s^2 \,+\, r_\odot^2 \,-\, 2\, s\, r_\odot \cos b \cos \ell}$. The solid angle window subtended from reciver to source event is written as $\mathrm{d}\Omega = \mathrm{d}\,(\sin b)\,\mathrm{d}\ell$.

4.3 Attenuation

While we have gotten our prompt flux component there are a couple additional caveats to deal with. Although high energy gamma rays have incredible penetrating power and allow for line of sight integration ,the issue rises when it interacts with other photons as it traverses galactic scales. Especially for heavy dark matter, the γ ray flux will suffer an exponential attenuation in the Sub-PeV to PeV range[64]. This happens due to pair production with photon baths [64].

$$\gamma\gamma_b \longrightarrow e^- e^+ \tag{33}$$

Here the γ_b refers to:-

- Starlight(SL) + Infrared(IR), which are active at lower energy scales.
- Cosmic Microwave Background(CMB) , which are dominant at $\sim$ PeV scales and above.

Thus for our case of a 1000 TeV photon source from within our galaxy we will only choose attenuation by CMB photon, as evidenced by the graph[64].

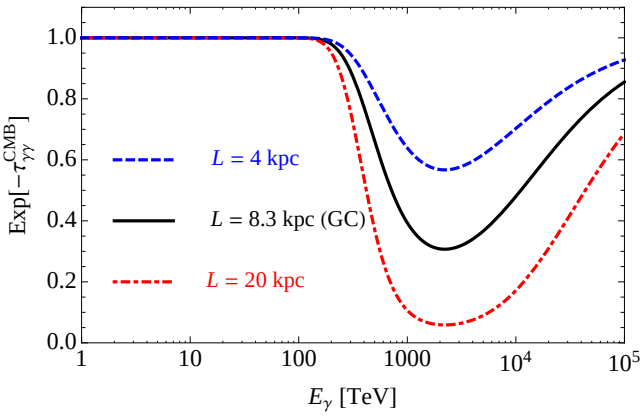

Figure 4.2: Measure of Attenuation for CMB processes [8]

For our case of pair production on CMB photons, the optical depth[19] through a traversal distance L can be given as :-

$$\tau_{\gamma\gamma}^{\rm CMB}(E_\gamma, L) = L \iint \sigma_{\gamma\gamma}(E_\gamma, \varepsilon)\, n_{\rm CMB}(\varepsilon)\, \frac{1-\cos\theta}{2} \sin\theta \mathrm{d}\theta\, \mathrm{d}\varepsilon\ , \tag{34}$$

where $\sigma_{\gamma\gamma}$, process cross-section :-

$$\sigma_{\gamma\gamma} = \frac{\pi}{2}\frac{\alpha^2}{m_e^2}(1-\beta^2)\left[(3-\beta^4)\ln\left(\frac{1+\beta}{1-\beta}\right) - 2\beta(2-\beta^2)\right]\ , \tag{35}$$

here,

$$\beta = \sqrt{1-1/s} \quad , \text{ and } \quad s = \frac{\varepsilon E_\gamma}{2m_e^2}(1-\cos\theta)\,, \tag{36}$$

Here, α is the fine-structure constant, m_e mass of electron, and θ the inter photon angle. $n_{\rm CMB}(\varepsilon)$, the differential number density for the CMBR is as follows.

$$n_{\rm CMB}(\varepsilon) = \frac{\varepsilon^2}{\pi^2}\frac{1}{e^{\varepsilon/T_{\rm CMB}}-1}\ , \tag{37}$$

[19] while the attenuation is of the form $\mathbf{e}^{-\tau}$, τ is known as the optical depth

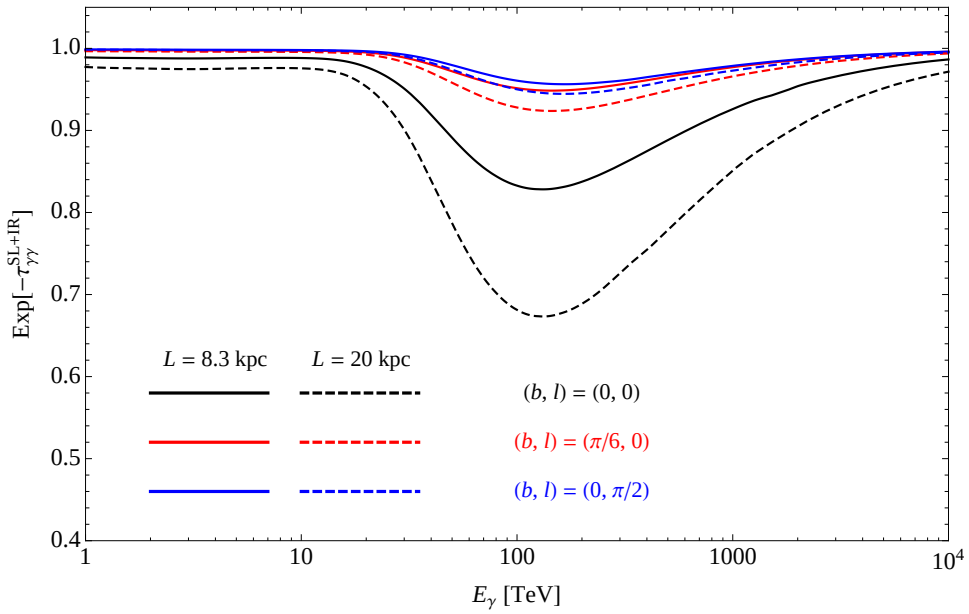

Figure 4.3: Measure of Attenuation for starlight(SL) and infrared(IR) processes [8]

where $T_{\rm CMB} = 2.348 \times 10^{-4}$ eV. Using the following parametrization $\varepsilon \to \varepsilon_c$; $\varepsilon_c = \sqrt{\varepsilon E_\gamma (1-\cos\theta)/2}$ the optical depth can be found numerically through a singular integral.

$$\tau_{\gamma\gamma}^{\rm CMB}(E_\gamma, L) = \frac{-4T_{\rm CMB}L}{\pi^2 E_\gamma^2} \int_{m_e}^{\infty} \varepsilon_c^3 \, \sigma_{\gamma\gamma}(\varepsilon_c) \ln\left[1 - e^{-\frac{\varepsilon_c^2}{E_\gamma T_{\rm CMB}}}\right] {\rm d}\varepsilon_c \, . \tag{38}$$

4.4 Secondary Processes

Electro-Weak Bremmsstrahlung

The incoming gamma ray flux can be changed due to bremmsstrahlung processes in annihilation channel via charged W or Neutral Z bosons [10] As shown in the image, this particular decay of a charge particle to a W/Z boson is inevitable if the original process must exist. This can lead to further production of additional secondary photons that must be shown as electro-weak radiative correction to our prompt flux [64]. While a

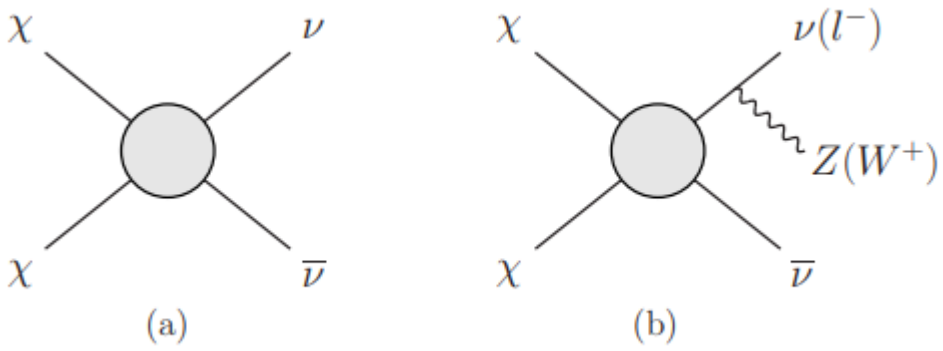

Figure 4.4: Bremmsstrahlung Process [10]

deeper study into these processes would make for a much more comprehensive study, it is unfortunaely beyond it's scope. Luckily, the coding mathematica package PPPC4DMID [11] used in our calculations, includes the EW corrections.

Inverse Compton Scattering

The other major process that happens involves the upscattering of low energy galactic photons through DM decay channels involving e^+e^-. This is referred to as Inverse Compton Scattering(ICS) and is studied as per [11]

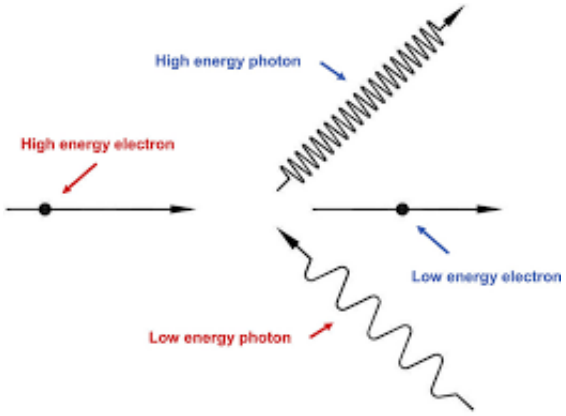

Figure 4.5: ICS process - upscattering [5]

The change to the prompt photon final states via ICS is given by,

$$\left.\frac{\mathrm{d}N_\gamma}{\mathrm{d}E_\gamma}\right|_{\mathrm{IC}}(E_\gamma) = \frac{1}{E_\gamma}\int_{m_e}^{m_{\mathrm{DM}}/2}\mathrm{d}E_e\,\frac{1}{b(E_e)}\,P_{\mathrm{IC}}(E_e,E_\gamma)\,\frac{\mathrm{d}N_e}{\mathrm{d}E_e}(E_e)\,. \tag{39}$$

Here, $\mathrm{d}N_e/\mathrm{d}E_e$ is the $e^{\pm}$ energy spectrum from DM decay and P_{IC} is the ICS power spectrum.

4.5 Total Photon Flux

Combining everything we have done so far, we can now write our total photon flux as,

$$\begin{aligned}\frac{d^2\phi_\gamma}{dE_\gamma d\Omega}(E_\gamma) &= \frac{1}{\Delta\Omega}\int_{\Delta\Omega}d\Omega\frac{1}{4\pi m_\chi\tau_\chi}\left(\frac{dN_\gamma}{dE_\gamma}+\frac{\mathrm{d}N_\gamma}{\mathrm{d}E_\gamma}|_{\mathrm{IC}}\right)(E_\gamma) \\ &\quad \int_0^{s_{\max}}\rho_\chi(s,b,l)\,e^{-\tau_{\gamma\gamma}(E_\gamma,s,b,\ell)}ds,\end{aligned} \tag{40}$$

5 Results

In this chapter we'll outline the approach taken with our calculations especially with the PPPC4DMID [11] spectra all the way to gain We re-write our total flux in terms ingredients from the public source code.

$$\frac{d\Phi_\gamma}{dE}(E_\gamma) = \frac{r_\odot}{4\pi}\frac{\rho_\odot}{M_{\rm DM}}\bar{J}\,\Delta\Omega\sum_f \Gamma_f \frac{dN_\gamma^f}{dE_\gamma} \tag{41}$$

Here every element of this is given as part of the PPPC4DMID, and thanks to [106], we can conveniently take our decay width out as τ_χ^{-1} since the Inverse Compton halo function ~ 1 at our high energy scales. Now that we have our total flux from the designed model and the chosen energy bin for the gamma ray event we can write out our estimator to calculate our upper limits.

5.1 The $\hat{\chi}^2$ Estimator

Given our data, new physics model and error bars, we can write the estimator as:

$$\hat{\chi}^2 = (data\ -\ N.P.model)^2/(\sigma)^2 \tag{42}$$

From here, we can estimate the minimal lower bound by ignoring the DM contribution. We can get our 95% CL limit from our core paper[12].

$$\hat{\chi}^2 - \hat{\chi}^2_{min} \equiv 2.71 \tag{43}$$

And this is the last piece of our puzzle.

5.2 Dark Matter lifetimes

Using the 95% CL limit, we can calculate the upper-limits on DM decay lifetimes for high energy scale through various channels and compare them against recent proposed limits.

Here we show 13 VHDM decay channels and the upper limits on their lifetime across the mass scale $10^6 - 10^8$ GeV.

The Y axis represent the lifetime as positive reals, multiplied by a factor of $10^{28} s$.

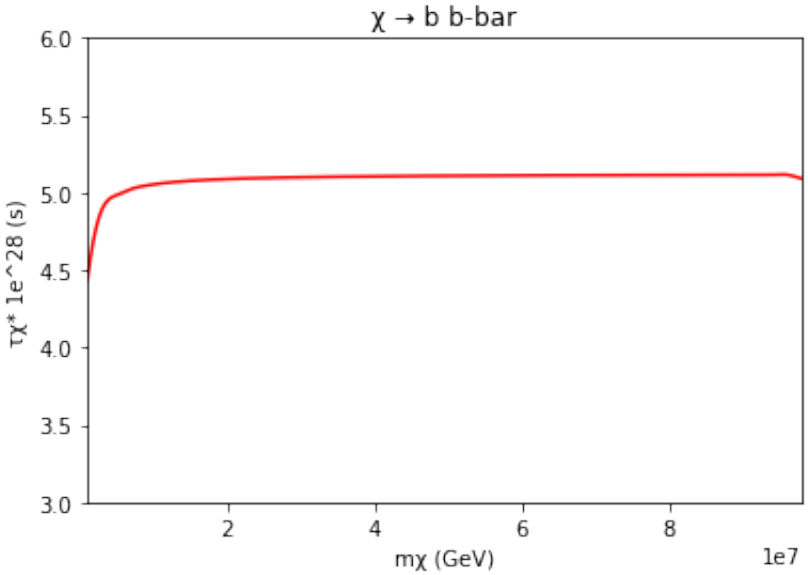

Figure 5.1: Upperlimits on VHDM lifetimes across sub-PeV scales as obtained from Tibet-AS$_\gamma$

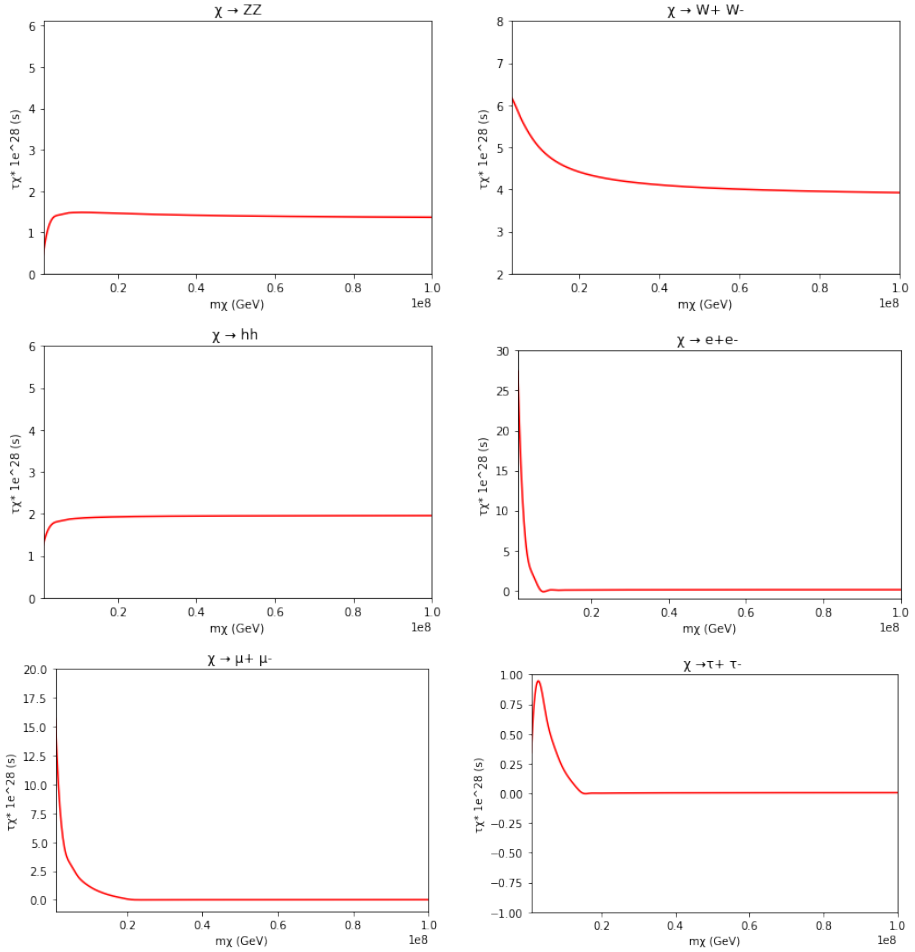

Figure 5.2: Upperlimits on VHDM lifetimes across sub-PeV scales as obtained from Tibet-AS$_\gamma$. Various Decay Channels shown

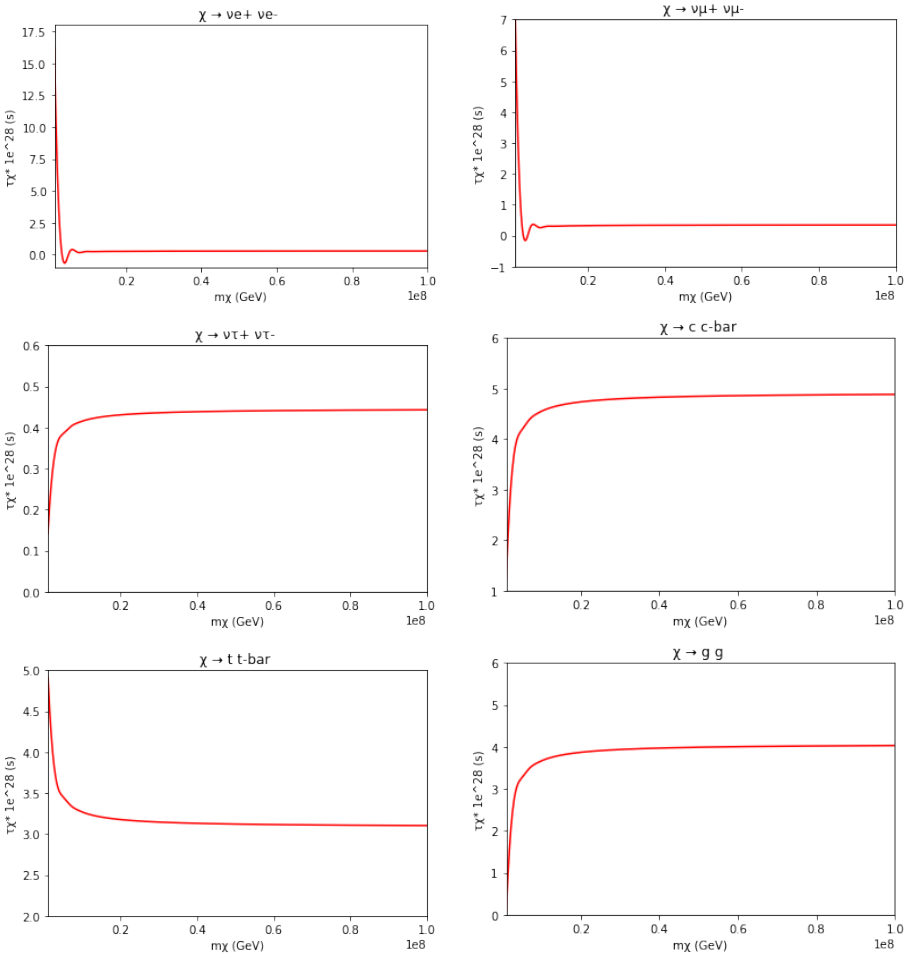

Figure 5.3: Upperlimits on VHDM lifetimes across sub-PeV scales as obtained from Tibet-AS$_\gamma$. Various Decay Channels shown

6 Discussion and Conclusion

The upperlimits of the DM mass lifetimes using the 95% confidence limit from [12] have been plotted in the previous section. Given that we have stripped back some of the rigour involved in the calculation it makes sense that we haven't gotten smoother s or more stringent lifetimes as expected. Nonetheless, all the values are in the general ball park and order of $[10^26, 10^28]$ seconds.

Now while the curves themselves leave much to be desired, several aspects point towards the lack of accuracy in the reproduction of data. The two major ones lie in the ignoring of background and the other the our choice of spectra usage. In the original work, the cosmic ray background models as shown in the sky region flux in chapter 4 were included in the estimator. While this would normally on it's own not produce a huge difference, it has definitely affected the shape of our curves. However certain salient features are still present. For instance, if you look at the $\chi \rightarrow b\bar{b}$ channel. Similar to the original work, the graph follows a pathway wit a rise towards the center. However, there isn't enough curvature. This may point to the lack of background data and consequently propagated errors in the confidence limit itself.

The other major issue which becomes very prevalent especially at these high mass scales is the PPPC4DMID spectra [11]. While the spectra boast more available functions and usability compared to HDM, it was simply not built for these mass scales. The flux function and other ingredients are built as interpolations within the already measured full spectra. However our starting mass range of $\sim 10^6 GeV$ is already outside this limit. As such the function had to extrapolate for every major calculation involved. This definitely affected the accuracy of the code.

From an author standpoint, perhaps combining the previous limits to display where

the current one lies would've helped validate the method further. However this involved tedious statistical calculations that are well beyond the scope of this thesis.

Going past the obvious shortcomings, this study showed all the necessary ingredient to tackle dark matter indirect detection via cosmic gamma rays. The Tibet AS_γ survey holds an unbelievable golden egg when it comes to dark matter studies right now. And given the high energy range and sky region($25^\circ < l < 100^\circ$) this has also allowed us to comfortably take several valid assumptions. We know that due to the distance from the superheavy galactic center, our current constraints are practically DM profile independent. Further more, the actual attenuation factor is quite low due to only having CMB interactions at those length scales. This lets the only point of doubt in our whole approach our New physics model and thus with further studies we should be easily able to give more stringent constraints.

Thus, these high energy gamma rays have given us fantastic insight into the the astrophysics of the MiklyWay galaxy. With these sub-PeV diffuse gamma rays, despite our simplifications we are able to get strong stable bounds in the ball park of the current strongest available limits [12]. With better spectra, and improved calculations, these results will definitely open up the way to probe heavy dark matter models via cosmic gamma rays and eventually may even lead to signals that point to particulate dark matter.

7 Appendix: Estimating DM Freezeout

We have mentioned in previous chapters that DM is a thermal relic and is freezed out in our current epoch. Here we will estimate this freezeout density and allude to why we call it a WIMP miracle.

We'll consider the simplest thermal relic scenario, where a single DM species annihilates to SM particles with velocity-independent σv_{rel}. We'll impose our current relic density measurements on this minimal scenario.

Assuming comoving volume is constant under no annihilation; if n is the physical (not comoving) DM number density, we would have

$$\frac{d}{dt}(na^3) = 0 \tag{44}$$

, where a is the scale factor. Expanding this out, we obtain

$$dn/dt + 3(\dot{a}/a)n = 0 \tag{45}$$

$$dn/dt + 3Hn = 0 \tag{46}$$

where $H = \dot{a}/a$ is the Hubble parameter.

Now integrating annihilation back into our equation the number density is additionally depleted, yielding:

$$\frac{dn}{dt} + 3Hn = -\frac{n^2}{2}\langle\sigma v_{\text{rel}}\rangle \times 2, \tag{47}$$

for indistinguishable annihilating particles.

The factor 2 occurs from counting two particles per annihilation. The $\langle\sigma v_{\text{rel}}\rangle$ indi-

cates an averaged cross-section over the DM velocity distribution.

However, given that this is a thermal process with a non-zero chemical potential, the inverse reaction – non-DM particles colliding to produce DM particles – can also occur in principle. Thus we modify our eqn as such,

$$\frac{dn}{dt} + 3Hn = -n^2\langle\sigma v_{\text{rel}}\rangle + \text{contribution from DM production}, \tag{48}$$

Assuming that there is a critical point for this dynamic process at equilibrium we we can write the DM-production term as $n_{\text{eq}}^2\langle\sigma v_{\text{rel}}\rangle$, where n_{eq} is the number density of the DM when it is in chemical equilibrium with its annihilation products.
So overall we have:

$$\frac{dn}{dt} + 3Hn = (n_{\text{eq}}^2 - n^2)\langle\sigma v_{\text{rel}}\rangle. \tag{49}$$

Let us now being our estimation by assuming that the DM must also be in equillibrium with the SM thermal bath.

Now, its equilibrium number density is given by $n_{\text{eq}} \sim (m_{\text{DM}}T)^{3/2}e^{-m_{\text{DM}}/T}$ when $T \ll m_{\text{DM}}$, and $n_{\text{eq}} \sim T^3$ where $T \gg m_{\text{DM}}$.

At zero annihilation rate, n evolves as $1/a^3$; at large rates, n will be forced close to n_{eq}. Here we can comfortable see that the a crossover occurs between the two regimes at $\langle\sigma v_{\text{rel}}\rangle n^2 \sim Hn$, i.e. $n\langle\sigma v_{\text{rel}}\rangle \sim H$.

Thus if you notice the DM density diverges from its equilibrium value, approaching the constant comoving density that we measure at late times, especially when the Hubble expansion time becomes comparable to the time needed for a given DM particle to annihilate. We refer to this point as “freezeout”.

A precise calculation of the DM relic abundance requires numerically solving the

evolution equation (eq. 49). This involves accounting for the non-trivial temperature evolution of the SM thermal bath when the number of relativistic degrees of freedom is changing. An recent iteration of this solution is given in Ref. [107].

Luckily, a simple estimate can be performed by neglecting these effects. We assume that freezeout is abrupt and occurs when $H = n_{\text{eq}}\langle\sigma v_{\text{rel}}\rangle$, that n tracks n_{eq} up to this point, after which the DM evolution follows a^{-3}. Let's denote the temperature of the universe at freezeout by T_f and define the new variable $x \equiv m_{\text{DM}}/T$. With this we can write $x_f \equiv m_{\text{DM}}/T_f$. Now the late-time DM number density is given by ,

$$n_{\text{today}} \approx n_{\text{eq}}(T_f)a(T_f)^3/(a_{\text{today}})^3 \tag{50}$$

Again there are broadly two cases to be considered; in the first case, the relativistic "hot relic". In this case $n_{\text{eq}}(T_f)a(T_f)^3$ is determined entirely by the number of degrees of freedom of the DM, and is almost independent of the freezeout temperature. This would imply that it would follow similarities toward remnant photon number density in the universe since the DM was originally that of a relativistic species and it has only been diluted by the cosmic expansion, not by any other number-changing effects. [20] This would as mentioned in chapter one suggest a DM mass around the eV scale, since the photon abundance is roughly $2 \times 10^9 \times$ larger than the baryon abundance, the energy density in baryons is comparable to that in DM, and the mass of a proton is 1 GeV. A scenario where hot DM constitutes 100% of the DM would lead to dramatic changes to structure formation, and is not consistent with observations (see e.g. Ref. [109], or Ref. [110] for more recent constraints).

[20] This conclusion may be evaded if there are large changes in the number of relativistic degrees of freedom coupled to DM and/or the SM between freezeout and the present day, that affect the two sectors differently, e.g. Ref. [108].

In the second case, freezeout occurs when the DM is non-relativistic. This scenario helps explain the difference in number density between DM and photons at freezeout, $n_{\text{eq}} \sim (m_{\text{DM}} T_f)^{3/2} e^{-m_{\text{DM}}/T_F}$ is exponentially suppressed.

Our condition for freezeout in this second scenario is thus that

$H \sim (m_{\text{DM}} T_f)^{3/2} e^{-m_{\text{DM}}/T_F} \langle \sigma v_{\text{rel}} \rangle$. Assuming freeze-out during the radiation dominated era we have, $H^2 \propto \rho \propto T^4$, and thus $T \propto H^{1/2} \propto t^{-1/2}$ [21]Within our approximations, we can thus write $H = H(T = m_{\text{DM}}) x^{-2}$, where as previously $x = m_{\text{DM}}/T$.

Now the freezeout criterion then becomes:

$$\begin{aligned} H(x=1) x_f^{-2} &\sim (m_{\text{DM}}^2)^{3/2} x_f^{-3/2} e^{-x_f} \langle \sigma v_{\text{rel}} \rangle, \\ \Rightarrow e^{-x_f} &\sim \frac{x_f^{-1/2} H(x=1)}{m_{\text{DM}}^3 \langle \sigma v_{\text{rel}} \rangle}. \end{aligned} \tag{51}$$

Since the exponential scaling with x_f on the LHS is much faster than the power-law scaling on the RHS, as a lowest-order approximation we can write

$$x_f \sim \ln(m_{\text{DM}}^3 \langle \sigma v_{\text{rel}} \rangle / H(x=1)). \tag{52}$$

[22]

Ignoring changes to the effective degree of freedom, the photon number density and DM number density will both scale as $1/a^3$ after freezeout, we can then approximate $\rho_{\text{DM}}/n_\gamma = m_{\text{DM}} n_{\text{DM}}/n_\gamma$ at freezeout, and require that this match the observed late-time value.

Now by the same reasoning as above, $n_{\text{DM}}(x_f) \sim H(x=1) x_f^{-2} / \langle \sigma v_{\text{rel}} \rangle$, whereas

[21]Here we ignore any changes in the number of degrees of freedom contributing to the energy density of the universe).

[22]Note that x_f has only a logarithmic dependence on the DM mass and the annihilation cross section.

$n_\gamma(x_f) \sim T_f^3 \sim m_{\rm DM}^3/x_f^3$. Thus we can write:

$$\frac{m_{\rm DM} n_{\rm DM}}{n_\gamma}(x_f) \sim \frac{H(T = m_{\rm DM})}{m_{\rm DM}^2} \frac{x_f}{\langle \sigma v_{\rm rel} \rangle}. \tag{53}$$

Since $H \propto T^2$, $H(T = m_{\rm DM})/m_{\rm DM}^2$ is approximately independent of $m_{\rm DM}$; writing $H \sim T^2/m_{\rm Planck}$, we can write:

$$\frac{\rho_{\rm DM}}{n_\gamma}(x_f) \sim \frac{1}{m_{\rm Planck}} \frac{x_f}{\langle \sigma v_{\rm rel} \rangle}. \tag{54}$$

Here x_f is roughly independent of $m_{\rm DM}$ at lowest order. So by fixing $\rho_{\rm DM}/n_\gamma$ to its measured present-day value we can also fix $\langle \sigma v_{\rm rel} \rangle$, to a value that is approximately independent of the DM mass.

Now let us put in some numbers: the DM mass density is roughly $5\times$ the baryon mass density, or ~ 5 GeV $\times n_b \sim 5 \times n_\gamma \times 5 \times 10^{-10}$ GeV, since the baryon-to-photon ratio is $\sim 5 \times 10^{-10}$. Since $m_{\rm Planck} \sim 10^{19}$ GeV, we obtain:

$$\begin{aligned} &\rho_{\rm DM}/n_\gamma \sim 3 \times 10^{-9} \text{GeV} \sim \frac{x_f}{\langle \sigma v_{\rm rel} \rangle} 10^{-19} \text{GeV}^{-1} \\ &\Rightarrow \langle \sigma v_{\rm rel} \rangle \sim x_f \times 10^{-10.5} \text{GeV}^{-2}. \end{aligned} \tag{55}$$

Since x_f is a log quantity, let us have a $\mathcal{O}(1)$ ansatz. if we take $\langle \sigma v_{\rm rel} \rangle \sim \alpha_D^2/m_{\rm DM}^2$, and choose $\alpha_D \sim 0.01$ to be comparable to the electroweak coupling of the SM, we infer that $m_{\rm DM} \sim 10^3$ GeV yields approximately the right relic abundance.

Building upon this, x_f:

$$\begin{aligned} x_f &\sim \ln(m_{\text{DM}}^3 \langle \sigma v_{\text{rel}} \rangle / H(x=1)) \\ &\sim \ln(m_{\text{DM}} m_{\text{Planck}} \langle \sigma v_{\text{rel}} \rangle) \\ &\sim \ln(10^{22}\text{GeV}^2 \times 10^{-10.5}\text{GeV}^{-2}) \\ &\sim 25. \end{aligned} \tag{56}$$

Substituting this back into our expression for $\langle \sigma v \rangle$ yields $\langle \sigma v_{\text{rel}} \rangle \sim 10^{-9}\text{GeV}^{-2} \sim 10^{-26}$ cm^3/s, and a natural mass scale for m_{DM} around a few hundred GeV.

A more careful calculation (e.g. Ref. [107]) gives $\langle \sigma v_{\text{rel}} \rangle \approx 2 - 3 \times 10^{-26}$ cm^3/s, almost independent of the DM mass; this cross section is known as the "thermal relic" cross section.

Now if you notice, this is the expected rate for a new particle in the 100 GeV mass range that interacts via the electroweak force. eg:- The Higgs Boson mass is 125GeV

Because supersymmetric extensions of the Standard Model of particle physics readily predict a new particle with these properties, this apparent coincidence is known as the "WIMP miracle"

References

[1] M. Persic, P. Salucci and F. Stel, *The Universal rotation curve of spiral galaxies: 1. The Dark matter connection*, *Mon. Not. Roy. Astron. Soc.* **281** (1996) 27, [astro-ph/9506004].

[2] S. Profumo, *An Introduction to Particle Dark Matter*. World Scientific, 2017, 10.1142/q0001.

[3] A. Arbey and F. Mahmoudi, *Dark matter and the early universe: A review*, *Progress in Particle and Nuclear Physics* (apr, 2021) 103865.

[4] E. L. Wright, X. Chen, N. Odegard, C. L. Bennett, R. S. Hill, G. Hinshaw et al., *FIVE-YEAR iWILKINSON MICROWAVE ANISOTROPY PROBE/i OBSERVATIONS: SOURCE CATALOG*, *The Astrophysical Journal Supplement Series* **180** (feb, 2009) 283–295.

[5] "Imagine the universe!." https://imagine.gsfc.nasa.gov/observatories/technology/gammaray_detectors2.html.

[6] A. López-Oramas, *Multi-year campaign of the gamma-ray binary ls i +61◦ 303 and search for vhe emission from gamma-ray binary candidates with the magic telescopes*, 04, 2015. 10.13140/RG.2.1.4140.4969.

[7] "The highest energy gamma rays discovered by t | eurekalert!." https://www.eurekalert.org/news-releases/771669#:~:text=The%20Tibet%20ASgamma%20experiment%2C%20a,to%20an%20estimated%20450%20TeV.

[8] M. Amenomori, Y. Bao, X. Bi, D. Chen, T. Chen, W. Chen et al., *First detection of sub-PeV diffuse gamma rays from the galactic disk: Evidence for ubiquitous*

galactic cosmic rays beyond PeV energies, *Physical Review Letters* **126** (apr, 2021) .

[9] R. Bartels, D. Gaggero and C. Weniger, *Prospects for indirect dark matter searches with MeV photons*, *Journal of Cosmology and Astroparticle Physics* **2017** (may, 2017) 001–001.

[10] N. F. Bell, J. B. Dent, T. D. Jacques and T. J. Weiler, *Electroweak bremsstrahlung in dark matter annihilation*, *Physical Review D* **78** (oct, 2008) .

[11] M. Cirelli, G. Corcella, A. Hektor, G. Hütsi, M. Kadastik, P. Panci et al., *PPPC 4 DM ID: a poor particle physicist cookbook for dark matter indirect detection*, *Journal of Cosmology and Astroparticle Physics* **2011** (mar, 2011) 051–051.

[12] T. N. Maity, A. K. Saha, A. Dubey and R. Laha, *Search for dark matter using sub-PeV γ-rays observed by Tibet ASγ*, 2105.05680.

[13] Wikipedia contributors, *Dark matter — Wikipedia, the free encyclopedia*, 2022.

[14] L. Gu, J. Mao, J. de Plaa, A. J. J. Raassen, C. Shah and J. S. Kaastra, *Charge exchange in galaxy clusters*, *Astronomy &amp Astrophysics* **611** (mar, 2018) A26.

[15] M. Milgrom, *MOND vs. dark matter in light of historical parallels*, *Studies in History and Philosophy of Science Part B: Studies in History and Philosophy of Modern Physics* **71** (aug, 2020) 170–195.

[16] A. Mahdavi, H. Hoekstra, A. Babul, D. D. Balam and P. L. Capak, *A dark core in abell 520*, *The Astrophysical Journal* **668** (oct, 2007) 806–814.

[17] Z. K. Silagadze.

[18] J.-W. Lee, S. Lim and D. Choi, *Bec dark matter can explain collisions of galaxy clusters*, 2008. 10.48550/ARXIV.0805.3827.

[19] D. Clowe, M. Markevitch, M. Bradač, A. H. Gonzalez, S. M. Chung, R. Massey et al., *ON DARK PEAKS AND MISSING MASS: A WEAK-LENSING MASS RECONSTRUCTION OF THE MERGING CLUSTER SYSTEM a520,*, *The Astrophysical Journal* **758** (oct, 2012) 128.

[20] A. J. Galea, *Interacting dark matter: Decay and bremsstrahlung processes*, Jan, 1970.

[21] S. M. Carroll, *Spacetime and Geometry*. Cambridge University Press, 7, 2019.

[22] S. Chen, G. W. Gibbons, Y. Li and Y. Yang, *Friedmann's equations in all dimensions and chebyshev's theorem*, *Journal of Cosmology and Astroparticle Physics* **2014** (dec, 2014) 035–035.

[23] M. Maggiore, *A Modern introduction to quantum field theory*. 2005.

[24] V. F. Mukhanov, H. A. Feldman and R. H. Brandenberger, *Theory of cosmological perturbations*, **215** (June, 1992) 203–333.

[25] D. H. Lyth and A. Riotto, *Particle physics models of inflation and the cosmological density perturbation*, *Physics Reports* **314** (jun, 1999) 1–146.

[26] A. R. Liddle and D. H. Lyth, *The cold dark matter density perturbation*, *Physics Reports* **231** (aug, 1993) 1–105.

[27] K. A. Olive, *Inflation*, *Physics Reports* **190** (1990) 307–403.

[28] A. Linde, *Particle physics and inflationary cosmology*, .

[29] V. Springel, S. D. M. White, A. Jenkins, C. S. Frenk, N. Yoshida, L. Gao et al., *Simulations of the formation, evolution and clustering of galaxies and quasars*, *Nature* **435** (jun, 2005) 629–636.

[30] L. Bergström, P. Ullio and J. H. Buckley, *Observability of rays from dark matter neutralino annihilations in the milky way halo*, *Astroparticle Physics* **9** (aug, 1998) 137–162.

[31] A. V. Kravtsov, A. A. Klypin, J. S. Bullock and J. R. Primack, *The cores of dark matter–dominated galaxies: Theory versus observations*, *The Astrophysical Journal* **502** (jul, 1998) 48–58.

[32] J. F. Navarro, C. S. Frenk and S. D. M. White, *The structure of cold dark matter halos*, *The Astrophysical Journal* **462** (may, 1996) 563.

[33] B. Moore, T. Quinn, F. Governato, J. Stadel and G. Lake, *Cold collapse and the core catastrophe*, *Monthly Notices of the Royal Astronomical Society* **310** (dec, 1999) 1147–1152.

[34] D. Merritt, A. W. Graham, B. Moore, J. Diemand and B. Terzić, *Empirical models for dark matter halos. i. nonparametric construction of density profiles and comparison with parametric models*, *The Astronomical Journal* **132** (jan, 2006) 2685–2700.

[35] E. W. Kolb and M. S. Turner, *The Early Universe*, vol. 69. 1990, 10.1201/9780429492860.

[36] W. J. G. de Blok, A. Bosma and S. McGaugh, *Simulating observations of dark matter dominated galaxies: towards the optimal halo profile*, *Monthly Notices of the Royal Astronomical Society* **340** (apr, 2003) 657–678.

[37] G. Jungman, M. Kamionkowski and K. Griest, *Supersymmetric dark matter*, *Physics Reports* **267** (mar, 1996) 195–373.

[38] G. D'Amico, M. Kamionkowski and K. Sigurdson, *Dark matter astrophysics*, 2009. 10.48550/ARXIV.0907.1912.

[39] D. Hooper, *Tasi 2008 lectures on dark matter*, 2009. 10.48550/ARXIV.0901.4090.

[40] L. Bergström, *Dark matter evidence, particle physics candidates and detection methods*, *Annalen der Physik* **524** (aug, 2012) 479–496.

[41] J. L. Feng, *Dark matter candidates from particle physics and methods of detection*, *Annual Review of Astronomy and Astrophysics* **48** (aug, 2010) 495–545.

[42] G. Bertone, D. Hooper and J. Silk, *Particle dark matter: evidence, candidates and constraints*, *Physics Reports* **405** (jan, 2005) 279–390.

[43] H. Yüksel, J. F. Beacom and C. R. Watson, *Strong upper limits on sterile neutrino warm dark matter*, *Physical Review Letters* **101** (sep, 2008) .

[44] T. R. Slatyer, *Tasi lectures on indirect detection of dark matter*, 2017. 10.48550/ARXIV.1710.05137.

[45] J. Kraus, *Measurement of electron production from cosmic rays in the ATLAS detector*, 2010.

[46] S. Hayakawa, *Propagation of the Cosmic Radiation through Intersteller Space*, *Progress of Theoretical Physics* **8** (11, 1952) 571–572, [https://academic.oup.com/ptp/article-pdf/8/5/571/5221264/8-5-571.pdf].

[47] S. R. Kelner, F. A. Aharonian and V. V. Bugayov, *Energy spectra of gamma-rays, electrons and neutrinos produced at proton-proton interactions in the very high energy regime*, *Phys. Rev. D* **74** (2006) 034018, [astro-ph/0606058].

[48] A. Kappes, J. Hinton, C. Stegmann and F. A. Aharonian, *Potential Neutrino Signals from Galactic Gamma-Ray Sources*, *Astrophys. J.* **656** (2007) 870–896, [astro-ph/0607286].

[49] N. Gupta, *PeV gamma rays from interactions of ultra high energy cosmic rays in the milky way*, *Astroparticle Physics* **35** (mar, 2012) 503–507.

[50] P. Lipari and S. Vernetto, *Diffuse galactic gamma-ray flux at very high energy*, *Physical Review D* **98** (aug, 2018) .

[51] C. P. de los Heros, *Status, challenges and directions in indirect dark matter searches*, *Symmetry* **12** (oct, 2020) 1648.

[52] J. Wessén and J. Ruiz, *Bachelor thesis: Dark matter signatures in cosmic γ-rays*, 2012.

[53] I. V. Moskalenko, T. A. Porter and A. W. Strong, *Attenuation of very high energy gamma rays by the milky way interstellar radiation field*, *The Astrophysical Journal* **640** (mar, 2006) L155–L158.

[54] T. M. Venters, *CONTRIBUTION TO THE EXTRAGALACTIC GAMMA-RAY BACKGROUND FROM THE CASCADES OF VERY HIGH ENERGY GAMMA RAYS FROM BLAZARS*, *The Astrophysical Journal* **710** (feb, 2010) 1530–1540.

[55] S. Vernetto and P. Lipari, *Absorption of very high energy gamma rays in the milky way*, *Physical Review D* **94** (sep, 2016) .

[56] A. D. Angelis, G. Galanti and M. Roncadelli, *Transparency of the universe to gamma-rays*, *Monthly Notices of the Royal Astronomical Society* **432** (may, 2013) 3245–3249.

[57] R. Ruffini, G. V. Vereshchagin and S.-S. Xue, *Cosmic absorption of ultra high energy particles*, *Astrophysics and Space Science* **361** (jan, 2016) .

[58] K. Fang and K. Murase, *Multimessenger implications of sub-PeV diffuse galactic gamma-ray emission*, *The Astrophysical Journal* **919** (sep, 2021) 93.

[59] CASA-MIA collaboration, M. C. Chantell et al., *Limits on the isotropic diffuse flux of ultrahigh-energy gamma radiation*, *Phys. Rev. Lett.* **79** (1997) 1805–1808, [astro-ph/9705246].

[60] A. Borione, M. A. Catanese, M. C. Chantell, C. E. Covault, J. W. Cronin, B. E. Fick et al., *Constraints on gamma-ray emission from the galactic plane at 300 TeV*, *The Astrophysical Journal* **493** (jan, 1998) 175–179.

[61] W. D. Apel, J. C. Arteaga-Velá zquez, K. Bekk, M. Bertaina, J. Blümer, H. Bozdog et al., *KASCADE-grande limits on the isotropic diffuse gamma-ray flux between 100 TeV and 1 EeV*, *The Astrophysical Journal* **848** (oct, 2017) 1.

[62] K. Ishiwata, O. Macias, S. Ando and M. Arimoto, *Probing heavy dark matter decays with multi-messenger astrophysical data*, *Journal of Cosmology and Astroparticle Physics* **2020** (jan, 2020) 003–003.

[63] K. Murase, R. Laha, S. Ando and M. Ahlers, *Testing the dark matter scenario for PeV neutrinos observed in IceCube*, *Physical Review Letters* **115** (aug, 2015) .

[64] A. Esmaili and P. D. Serpico, *Gamma-ray bounds from EAS detectors and heavy decaying dark matter constraints*, *Journal of Cosmology and Astroparticle Physics* **2015** (oct, 2015) 014–014.

[65] A. Esmaili, S. K. Kang and P. D. Serpico, *IceCube events and decaying dark matter: hints and constraints*, *Journal of Cosmology and Astroparticle Physics* **2014** (dec, 2014) 054–054.

[66] O. Kalashev and M. Kuznetsov, *Constraining heavy decaying dark matter with the high energy gamma-ray limits*, *Physical Review D* **94** (sep, 2016) .

[67] M. Kachelrieß, O. Kalashev and M. Kuznetsov, *Heavy decaying dark matter and IceCube high energy neutrinos*, *Physical Review D* **98** (oct, 2018) .

[68] B. Feldstein, A. Kusenko, S. Matsumoto and T. T. Yanagida, *Neutrinos at IceCube from heavy decaying dark matter*, *Physical Review D* **88** (jul, 2013) .

[69] K. Harigaya, M. Ibe and T. T. Yanagida, *Lower Bound on the Garvitino Mass $m_{3/2} > O(100)$ TeV in R-Symmetry Breaking New Inflation*, *Phys. Rev. D* **89** (2014) 055014, [1311.1898].

[70] K. Harigaya, M. Kawasaki, K. Mukaida and M. Yamada, *Dark matter production in late time reheating*, *Physical Review D* **89** (apr, 2014) .

[71] A. Bhattacharya, R. Gandhi and A. Gupta, *The direct detection of boosted dark matter at high energies and PeV events at IceCube*, *Journal of Cosmology and Astroparticle Physics* **2015** (mar, 2015) 027–027.

[72] C. Rott, K. Kohri and S. C. Park, *Superheavy dark matter and IceCube neutrino signals: Bounds on decaying dark matter*, *Physical Review D* **92** (jul, 2015) .

[73] E. Dudas, Y. Mambrini and K. A. Olive, *Monochromatic neutrinos generated by dark matter and the seesaw mechanism*, *Physical Review D* **91** (apr, 2015) .

[74] Y. Daikoku and H. Okada, *PeV Scale Right Handed Neutrino Dark Matter in S_4 Flavor Symmetric extra U(1) model*, *Phys. Rev. D* **91** (2015) 075009, [1502.07032].

[75] C. E. Aisati, M. Gustafsson and T. Hambye, *New search for monochromatic neutrinos from dark matter decay*, *Physical Review D* **92** (dec, 2015) .

[76] L. A. Anchordoqui, V. Barger, H. Goldberg, X. Huang, D. Marfatia, L. H. da Silva et al., *Erratum: IceCube neutrinos, decaying dark matter, and the hubble constant [phys. rev. db92/b, 061301(r) (2015)]*, *Physical Review D* **94** (sep, 2016) .

[77] S. M. Boucenna, M. Chianese, G. Mangano, G. Miele, S. Morisi, O. Pisanti et al., *Decaying leptophilic dark matter at IceCube*, *Journal of Cosmology and Astroparticle Physics* **2015** (dec, 2015) 055–055.

[78] P. Ko and Y. Tang, *IceCube events from heavy DM decays through the right-handed neutrino portal*, *Physics Letters B* **751** (dec, 2015) 81–88.

[79] C. E. Aisati, M. Gustafsson, T. Hambye and T. Scarna, *Dark matter decay to a photon and a neutrino: The double monochromatic smoking gun scenario*, *Physical Review D* **93** (feb, 2016) .

[80] P. B. Dev, D. K. Ghosh and W. Rodejohann, *R-parity violating supersymmetry at IceCube*, *Physics Letters B* **762** (nov, 2016) 116–123.

[81] S. B. Roland, B. Shakya and J. D. Wells, *PeV neutrinos and a 3.5 keV x-ray line from a PeV-scale supersymmetric neutrino sector*, *Physical Review D* **92** (nov, 2015) .

[82] P. B. Dev, D. Kazanas, R. Mohapatra, V. Teplitz and Y. Zhang, *Heavy right-handed neutrino dark matter and PeV neutrinos at IceCube*, *Journal of Cosmology and Astroparticle Physics* **2016** (aug, 2016) 034–034.

[83] M. R. Fiorentin, V. Niro and N. Fornengo, *A consistent model for leptogenesis, dark matter and the IceCube signal*, *Journal of High Energy Physics* **2016** (nov, 2016) .

[84] P. D. Bari, P. O. Ludl and S. Palomares-Ruiz, *Unifying leptogenesis, dark matter and high-energy neutrinos with right-handed neutrino mixing via higgs portal*, *Journal of Cosmology and Astroparticle Physics* **2016** (nov, 2016) 044–044.

[85] M. Chianese, G. Miele and S. Morisi, *Interpreting IceCube 6-year HESE data as an evidence for hundred TeV decaying dark matter*, *Physics Letters B* **773** (oct, 2017) 591–595.

[86] O. Catà , A. Ibarra and S. Ingenhütt, *Dark matter decay through gravity portals*, *Physical Review D* **95** (feb, 2017) .

[87] A. Bhattacharya, R. Gandhi, A. Gupta and S. Mukhopadhyay, *Boosted dark matter and its implications for the features in IceCube HESE data*, *Journal of Cosmology and Astroparticle Physics* **2017** (may, 2017) 002–002.

[88] N. Hiroshima, R. Kitano, K. Kohri and K. Murase, *High-energy neutrinos from multibody decaying dark matter*, *Physical Review D* **97** (jan, 2018) .

[89] D. Borah, A. Dasgupta, U. K. Dey, S. Patra and G. Tomar, *Multi-component fermionic dark matter and IceCube PeV scale neutrinos in left-right model with gauge unification*, *Journal of High Energy Physics* **2017** (sep, 2017) .

[90] G. K. Chakravarty, N. Khan and S. Mohanty, *Supergravity model of inflation and explaining IceCube HESE data via PeV dark matter decay*, *Advances in High Energy Physics* **2020** (aug, 2020) 1–14.

[91] M. Chianese, G. Miele, S. Morisi and E. Peinado, *Neutrinophilic dark matter in the epoch of IceCube and fermi-LAT*, *Journal of Cosmology and Astroparticle Physics* **2018** (dec, 2018) 016–016.

[92] M. Dhuria and V. Rentala, *PeV scale supersymmetry breaking and the IceCube neutrino flux*, *Journal of High Energy Physics* **2018** (sep, 2018) .

[93] Y. Sui and P. B. Dev, *A combined astrophysical and dark matter interpretation of the IceCube HESE and throughgoing muon events*, *Journal of Cosmology and Astroparticle Physics* **2018** (jul, 2018) 020–020.

[94] G. Lambiase, S. Mohanty and A. Stabile, *PeV IceCube signals and dark matter relic abundance in modified cosmologies*, *The European Physical Journal C* **78** (apr, 2018) .

[95] M. Chianese and A. Merle, *A consistent theory of decaying dark matter connecting IceCube to the sesame street*, *Journal of Cosmology and Astroparticle Physics* **2017** (apr, 2017) 017–017.

[96] H. Kim and E. Kuflik, *Superheavy thermal dark matter*, *Physical Review Letters* **123** (nov, 2019) .

[97] J. Jaeckel and W. Yin, *Boosted neutrinos and relativistic dark particles as messengers from reheating*, *Journal of Cosmology and Astroparticle Physics* **2021** (feb, 2021) 044–044.

[98] M. A. G. Garcia, Y. Mambrini, K. A. Olive and S. Verner, *Case for decaying spin- 3/2 dark matter*, *Phys. Rev. D* **102** (2020) 083533, [2006.03325].

[99] A. Azatov, M. Vanvlasselaer and W. Yin, *Dark matter production from relativistic bubble walls*, 2021. 10.48550/ARXIV.2101.05721.

[100] T. Cohen, K. Murase, N. L. Rodd, B. R. Safdi and Y. Soreq, γ *-ray Constraints on Decaying Dark Matter and Implications for IceCube*, *Phys. Rev. Lett.* **119** (2017) 021102, [1612.05638].

[101] M. Chianese, D. F. Fiorillo, G. Miele, S. Morisi and O. Pisanti, *Decaying dark matter at IceCube and its signature on high energy gamma experiments*, *Journal of Cosmology and Astroparticle Physics* **2019** (nov, 2019) 046–046.

[102] A. Bhattacharya, A. Esmaili, S. Palomares-Ruiz and I. Sarcevic, *Update on decaying and annihilating heavy dark matter with the 6-year IceCube HESE data*, *Journal of Cosmology and Astroparticle Physics* **2019** (may, 2019) 051–051.

[103] P. Mollitor, E. Nezri and R. Teyssier, *Baryonic and dark matter distribution in cosmological simulations of spiral galaxies*, *Monthly Notices of the Royal Astronomical Society* **447** (12, 2014) 1353–1369, [https://academic.oup.com/mnras/article-pdf/447/2/1353/8093598/stu2466.pdf].

[104] T. K. Chan, D. Kereš , J. Oñorbe, P. F. Hopkins, A. L. Muratov, C.-A. Faucher-Giguère et al., *The impact of baryonic physics on the structure of dark matter haloes: the view from the FIRE cosmological simulations*, *Monthly Notices of the Royal Astronomical Society* **454** (oct, 2015) 2981–3001.

[105] M. Benito, F. Iocco and A. Cuoco, *Uncertainties in the galactic dark matter distribution: An update*, *Physics of the Dark Universe* **32** (may, 2021) 100826.

[106] M. Cirelli and P. Panci, *Inverse compton constraints on the dark matter excesses*, *Nuclear Physics B* **821** (nov, 2009) 399–416.

[107] G. Steigman, B. Dasgupta and J. F. Beacom, *Precise relic WIMP abundance and its impact on searches for dark matter annihilation*, *Physical Review D* **86** (jul, 2012) .

[108] S. Baek, P. Ko and W.-I. Park, *The 3.5 kev x-ray line signature from annihilating and decaying dark matter in weinberg model*, 2014. 10.48550/ARXIV.1405.3730.

[109] J. R. Primack and M. A. K. Gross, *Hot dark matter in cosmology*, 2000. 10.48550/ARXIV.ASTRO-PH/0007165.

[110] E. D. Valentino, E. Giusarma, M. Lattanzi, O. Mena, A. Melchiorri and J. Silk, *Cosmological axion and neutrino mass constraints from planck 2015 temperature and polarization data*, *Physics Letters B* **752** (jan, 2016) 182–185.